HYBRID DISTRIBUTED GENERATION SYSTEM (HDGS) MODELLING FOR SMART SELF-HEALING ELECTRIC MICROGRIDS

BY

HUSSEIN ABDELLATIF

A Thesis Presented to the

DEANSHIP OF GRADUATE STUDIES

KING FAHD UNIVERSITY OF PETROLEUM & MINERALS

DHAHRAN, SAUDI ARABIA

In Partial Fulfillment of the

Requirements for the Degree of

MASTER OF SCIENCE

In

ELECTRICAL ENGINEERING

January 2016

KING FAHD UNIVERSITY OF PETROLEUM & MINERALS

DHAHRAN- 31261, SAUDI ARABIA

DEANSHIP OF GRADUATE STUDIES

This thesis, written by HUSSEIN ABDELLATIF under the direction his thesis advisor and approved by his thesis committee, has been presented and accepted by the Dean of Graduate Studies, in partial fulfillment of the requirements for the degree of **MASTER OF SCIENCE IN ELECTRICAL ENGINEERING.**

Dr. MOHAMMAD ALMUHAINI
(Advisor)

Dr. ALI ALSHAIKHI
Department Chairman

Prof. IBRAHIM ELAMIN
(Member)

Prof. SALAM A. ZUMMO
Dean of Graduate Studies

Prof. MOHAMMAD ABIDO
(Member)

9/5/16
Date

DEDICATION

I would like to dedicate my thesis work to everyone who stood by my side and encouraged me. A special thanks to my family and my close friends. I dedicate this work first of all to my mother who eagerly wanted to see me at this stage, and my beloved dad who inspired me to move forward.

A special feeling of gratitude to my sisters who believed in me and who have always supported me.

I would also like to dedicate this work for my friend who supported me along the whole way from the beginning of my master degree until the end, Agnieszka Lukaszczyk. I would also like to give special thanks to my friend, Abdelrahman Mohammad.

ACKNOWLDGMENTS

Acknowledgment is due to the King Fahd University of Petroleum & Minerals for supporting this research.

I would like to express my appreciation to Dr. Mohammad AlMuhaini who served as my major advisor. I also would like to thank the members of my thesis committee Prof. Ibrahim ElAmin, and Prof. Mohammad Abido.

TABLE OF CONTENTS

Contents

ACKNOWLDGMENTS ..... **V**

TABLE OF CONTENTS ..... **VI**

LIST OF TABLES ..... **IX**

LIST OF FIGURES ..... **X**

LIST OF ABBREVIATIONS ..... **XI**

NOMENCLATURE ..... **XIV**

ABSTRACT (ENGLISH) ..... **XIX**

ABSTRACT (ARABIC) ..... **XXI**

CHAPTER 1 INTRODUCTION **1**

1.1 Smart Self-Healing Microgrids **1**

1.2 Motivation **2**

1.3 Objectives **3**

1.4 Thesis Organization **4**

CHAPTER 2 LITERATURE REVIEW **5**

2.1 Distributed Generation **5**

2.2 The PV System **7**

2.3 The Wind Turbine Generator (WTG) **9**

2.4 Data Forecast Techniques and Simulations....10
2.5 Smart Grids....12
2.6 Reliability of Microgrids....13
CHAPTER 3 PROBLEM FORMULTION AND INPUT DATA....14
3.1 Modelling the Renewable Resources....14
3.1.1 The Operational Model of the PV System....15
3.1.2 The Operational Model of the WTG....19
3.2 The Model of the Conventional DG....22
3.3 The Model of the Energy Storage System....23
3.4 The Operational Model of the HDGS....29
3.5 Auto Regressive Moving Average Representation....33
3.6 Monte Carlo Simulation....34
3.7 Cost Analysis for the Subsystems....35
3.8 Physical Modelling of Renewables....38
3.9 Reliability Modelling and Markov States....41
3.10 The Comprehensive Model of the HDGS....45
CHAPTER 4 CASE STUDIES AND SIMULATIONS....46
4.1 The HDGS's Data Forecast....46
4.2 Case Studies....56
4.2.1 Case 1: Supplying a local load during interruptions....56
4.2.2 Case 2: Supplying a local load and a nearby load during interruptions....60
4.2.3 Case 3: Supplying two loads during interruptions based upon a priority list....62
4.2.4 Case 4: The Diesel Generator's Parameter....66

4.2.5 Case 5: The Battery's Parameter 67

4.3 Discussion and Analysis 69

CHAPTER 5 CONCLUSION AND FUTURE WORK 71

5.1 Conclusion 71

5.2 Future Work 72

APPENDIX A INPUT DATA AND PARAMETERS 73

REFERENCES 76

VITAE 82

LIST OF TABLES

Table 3-1 Variable Definitions 28
Table 4-1 Final Failure Rate And Repair Time [67] 46
Table 4-2 Statistical and Reliability Data Summary (During Failures) 64
Table 4-3 case study analysis (Case 4) 67
Table 4-4 case study analysis (Case 5) 68
Table A-1 Efficiency and Other Parameters 73
Table A-2 WTG Failure Rates and Repair Times [19], [39]-[40] 73
Table A-3 PV System Components' Failure and Repair Rates [19],[67] 74
Table A-4 Units' Costs [23] 74
Table A-5 PV System's Parameters [41] 75
Table A-6 WTG System's Parameters [41] 75
Table A-7 Conventional DG System's Parameters [41], [68] 75

LIST OF FIGURES

Figure 3-1 The Operational Model of the PV System 15
Figure 3-2 The Operational Model of the Wind System 20
Figure 3-3 The Operational Model of the Conventional System 23
Figure 3-4 The Operational Model of the Storage System 24
Figure 3-5 Flowchart of the Flow of Energy 26
Figure 3-6 Diesel Generator's Energy Flow Incorporation into The System 27
Figure 3-7 The Operational Connection of The HDGS 32
Figure 3-8 The Physical Model of the PV DG 39
Figure 3-9 An Advanced PV Physical Model 39
Figure 3-10 The Physical Model of the Wind DG 40
Figure 3-11 Connection from the WTG to the Load 41
Figure 3-12 The General/Subsystem Reliability Model 42
Figure 3-13 The Reliability Model of the Conventional DG 42
Figure 3-14 Markov model of the PV Strings 43
Figure 3-15 The Complete Detailed HDGS 45
Figure 4-1 Yearly Average Solar Radiation, Metrological 48
Figure 4-2 Forecasted Yearly Average Solar Radiation 48
Figure 4-3 Corrected Yearly Average Solar Radiation 49
Figure 4-4 Yearly Average Ambient Temperature 50
Figure 4-5 Forecasted Yearly Average Ambient Temperature 50
Figure 4-6 Corrected Yearly Average Ambient Temperature 51
Figure 4-7 Yearly Average Wind Speed 52
Figure 4-8 Forecasted Yearly Average Wind Speed 52
Figure 4-9 Corrected Yearly Average Wind Speed 53
Figure 4-10 Yearly Average Solar Power 54
Figure 4-11 Yearly Average Wind Power 54
Figure 4-12 Wind Speed Vs. Wind Power 55
Figure 4-13 Yearly Average Load Power 55
Figure 4-14 Case 1 Representation 57
Figure 4-15 Case 2 Representation 57
Figure 4-16 Case 3 Representation 58
Figure 4-17 Case 1: Power Flow During Failures 58
Figure 4-18 Case 2: Power Flow During Failures (Load 1) 61
Figure 4-19 Case 2: Power Flow During Failures (Load 2) 61
Figure 4-20 Case 3: Power Flow During Failures (Load 1) 63
Figure 4-21 Case 3: Power Flow During Failures (Load 2) 63

LIST OF ABBREVIATIONS

HDGS: Hybrid Distributed Generation Systems

μG: Microgrid

DG: Distributed Generator

SOC: States of Charge

RBTS: Roy Billinton Test System

LOLP: Loss of Load Probability

FTA: Fault Tree Analysis

RBD: Reliability Block Diagrams

LOLE: Loss of Load Expectation

LOEE: Loss of Energy Expectation

LOLF: Loss of Load Frequency

ARMA: Auto Regressive Moving Average Method

AIC: Akaike Information Criteria

BIC: Bayesian Information Criteria

MTTF: Mean Time to Fail

MTTR: Mean Time to Repair

EDRC: Effective Descending Radiation Curve

DOD: Depth of Discharge

CB: Battery Capacity

NOCT: Normal Operating Cell Temperature of Module

STC: Standard Test Conditions of Module

FF: Fill Factor

SAIFI: System Average Interruption Frequency Index

SAIDI: System Average Interruption Duration Index

CAIDI: Customer Average Interruption Duration Index

ASAI: Average System Availability Index

ASUI: Average System Un-Availability Index

ENS: Energy Not Supplied

AENS: Average Energy Not Supplied

LP: Load Point

NPC: Net Present Cost

PWF: Present Worth Factor

NOMENCLATURE

Superscript * Denotes Measurement at Standard Test Conditions

Kc: Radiation Threshold Required for The PV Panels to Work Effectively

ηbat: Battery's Efficiency

ηinv: Inverter's Efficiency

E_B: Available Battery Bank Energy

EBmin: Minimum Battery Charge

EBmax: Maximum Battery Charge

E_D: Energy Load Demand

E_S: Energy for Storage

E_U: Unsatisfied Energy

E_{User}: Energy Supplied to User

E_{Unused}: Unused Energy (full battery)

$\emptyset_i$: AR Parameter of the Model

$\boldsymbol{\theta_j}$: MA Parameter of the Model

$\boldsymbol{\alpha_t}$: Normal White Noise with Zero Mean

$\boldsymbol{\sigma_a^2}$: Variance

G*: Irradiance at STC

Ta: Ambient Temperature

Tc: Operating Temperature of Module Above Ambient

Geff: Effective Irradiance, Related to Incidence Angle

σoc: Empirically Adjusted Parameter = ~.04

$\boldsymbol{G_{oc}}$: Empirically Adjusted Parameter = G*

Npv: Number of Modules

$\mathbf{K_I}$: Temperature Factor of the Short Circuit Current (in amperes/ Celsius)

$\mathbf{K_V}$: Open Circuit Voltage Temperature Factor

Cp: Power Coefficient

ρ: Air Density (1.225 kg/m^3)

V: Wind Velocity (m/sec)

A: Swept Area of Rotor Disc (m^2)

$\mathbf{I_j}$: Sum of All Present Capital Cost of a Unit j

S_{dj}: Salvage Value Expressed in the Present Time

X_j: Number of Generation Units

OM_{dj}: Present Cost of Operation and Maintenance

E_j: Energy Output of the jth Unit

I_r: Annual Interest Rate

i_F: Inflation Rate

CCU: Unit's Capital Cost

Ld: Unit's Life Time

xd: Number of Units Purchased in the Project's Life Time

S_{bt}: Salvage Value of the Last Unit Purchased

S_d: Salvage Value of a Unit

α_d: Capital Cost of a Unit

Rd: Unit's Capacity

S_{DG}: Size of Operation of the Conventional DG

DG_h: Hours of Operation of the Conventional DG

OMG: Costs of the Conventional DG

OMB: Battery of the Conventional DG

Sb: Size of the Battery

FC: Fuel Cost

MC: Maintenance Cost

Q: Radiation for the Titled panel

Θ: Latitude

Φ: Inclination of the Earth's Axis Toward the Sun

β: Angle at which the Sun Rises or Sets

Q: Coefficients Matrix

$\mathbf{P_{iup}}$: Steady State Probability of the ith Up

$\mathbf{P_{idn}}$: Steady State Probability of the ith Down

$\mathbf{f_{up}}$: Frequency of the Up States

$\mathbf{f_{dn}}$: Frequency of the Down States

μ: Overall Repair Rate of the Network with PV Installed

λ: Overall Failure Rate of the Network with PV Installed

r: Repair Time

ABSTRACT (ENGLISH)

Full Name : [HUSSEIN ADEL ABDELAZIM ABDELLATIF]

Thesis Title : [Hybrid Distributed Generation System (HDGS) Modelling for Smart Self-Healing Electric Microgrids]

Major Field : [Electrical Engineering]

Date of Degree : [January 2016]

Hybrid distributed generation systems (HDGSs) can be considered a future aspect of electric grids, and they are currently a rich field of research. There are numerous studies on renewable resources, mainly wind and PV. However, the amount of research on hybrid distributed generation systems (HDGSs) is not as abundant. There are multiple ways to model an HDGS depending on the method of the research, e.g., probabilistic or deterministic. The subsystems of an HDGS can be represented as states using Markov modelling, by simulation using the Monte Carlo technique, by mathematical equations, etc. In the present study, the subsystems of an HDGS will be modelled separately to achieve a highly accurate model for each by including the physical components of every subsystem.

This study proposes a new method of representing a HDGS in that it makes use of multiple techniques and simulations. An effective energy management technique with mathematical equations that govern the power exchange, locally and on the feeder, is also proposed, which gives the running of some energy sources priority over others to minimize the operational cost. Reliability block diagrams (RBDs) will be used to group every subsystem

into a minimal number of components to reduce calculation time and complexity. The metrological data of the solar radiation (SR), wind speed (WS), and ambient temperature (TEMP) will be collected and used for forecasting future data. As this study is primarily focused on the operation of the HDGS, the forecast will be an hourly sequential forecast using the auto regressive moving average (ARMA) technique. Secondly, the power output of each distributed generator (DG) will be obtained by using the input-output relation of each subsystem. Monte Carlo simulations will be used to simulate the failures of every subsystem in addition to the equivalent failures seen by the load from the grid. All the subsystems, including the storage, will then be combined into one HDGS. The proposed mathematical equations that govern the energy exchange between the HDGS and the load will subsequently be applied, taking into account the Monte Carlo simulation of all failures and repairs. Thus, the energy supplied to the load at every hour will be obtained as well as the excess or lack of energy at every hour. The three following cases will be studied: one in which the HDGS will supply only the local load beside it, one in which the HDGS will supply the local load and the next load if possible, and one in which the HDGS will supply two loads depending on a provided priority list. Lastly, the reliability of the system will be studied, and additional case studies and analyses will be undertaken.

ABSTRACT (ARABIC)

الاسم الكامل: حسين عادل عبدالعظيم عبداللطيف

عنوان الرسالة: نمذجة أنظمة توليد الطاقة الموزعة الهجينة لتطبيق خاصية استعادة الطاقة ذاتيا في شبكات الكهرباء الحديثة

التخصص: هندسة كهربائية

تاريخ الدرجة العلمية: يناير 2016

أنظمة توليد الطاقة الموزّعة هي مستقبل شبكات الكهرباء وهي أيضا مجال بحث غني في الوقت الحاضر. هناك العديد من الدراسات على مصادر الطاقة المتجددة، أهمها الطاقة الشمسية والمولدة بالرياح. ومع ذلك، فإن كثافة البحوث على أنظمة توليد الطاقة الموزعة ليس مثل تلك عن مصادر الطاقة المتجددة. هناك طرق عديدة لتمثيل أنظمة الطاقة الموزّعة وهذا يعتمد على الهدف من البحث. مصادر الطاقة اللتي تكون مثل هذه الأنظمة يمكن أن تُمثَّل كمستويات باستخدام نظام (ماركوف)، أو أن تُمثّل باستخدام طريقة (مونت كارلو)، أو أن تُمثّل كتدفّق للطاقة، إلى آخره. في هذه الدراسة، كل مصدر طاقة سيتم تمثيله على حدا للوصول إلى دقّة عالية لكل مصدر طاقة ولكل مكّون لهذا المصدر. رسوم الثقة التخطيطية ستسخدم لتجميع كل نظام فرعي في أصغر عدد ممكن من المكوّنات لتقليل تعقيد النظام ولتوفير وقت تحليل النظام. معلومات الأرصاد الجوية كشدة الإضاءة، سرعة الرياح، وحرارة الجو ستجمع وتستخدم لتوقع البيانات المستقبلية. بما أن هذه الدراسة هي لدراسة قصيرة المدى، توَقُّع البيانات سيكون بشكل متسلسل لكل ساعة باستخدام طريقة (ARMA). بعد ذلك، الطاقة المخرجة من كل مصدر طاقة موزّع ستحسب بناء على المعادلات الخاصة بكل مصدر طاقة. طريقة مونت كارلو ستسخدم لتمثيل معدل الفشل والإصلاح لكل نظام فرعي وأيضا لمعدلات الإخفاق والإصلاح التي يراها المستخدم عند اتصاله بشبكة الكهرباء. كل الأنظمة الفرعية بما فيها بطارية تخزين الطاقة سوف تجمع في نظام الطاقة الموزّعة. نظام تدفق الطاقة المقترح بين نظام الطاقة الموزّعة ونقاط استهلاك الطاقة سيطبّق آخذًا في الاعتبار البيانات الناتجة من محاكاة مونت كارلو. وبالتالي، سيتم الحصول على الطاقة المورّدة لنقاط الاستهلاك في كل ساعة وكذلك أي زيادة أو نقص في الطاقة في كل ساعة. ثلاث حالات سيتم دراستها: الأولى حيث نظام الطاقة الموزّعة سيورّد طاقة لنقطة الاستهلاك بجانبه فقط، والثانية حيث نظام الطاقة الموزّعة سيوّرد طاقة لنقطة الاستهلاك بجانبه والنقطة اللتي تليها إن أمكن، والثالثة حيث نظام الطاقة الموزّعة سيوّرد طاقة لنقطتي استهلاك تبعا لقائمة الأولوية المعطاة. وأخيرا، سيتم دراسة موثوقية النظام وسيتم إجراء تحليل لدراسة تأثير تغيير بعض العوامل في النظام على النظام ككل. وتقترح هذه الدراسة طريقة جديدة لتمثيل نظام

الطاقة الموزّعة وستستخدم تقنيات متعددة ومنها المحاكاة للقيام بذلك. والدراسة تقترح أسلوبًا فعّالًا لتدفّق الطاقة أيضا والذي يعطي الأولوية لتشغيل بعض مصادر الطاقة على الآخرين لتقليل التكلفة التشغيلية.

CHAPTER 1

INTRODUCTION

1.1 Smart Self-Healing Microgrids

Microgrids (μG) are becoming increasingly common in the electrical power field. They can be designed and modelled in different schemes and may work in parallel with the grid or in an islanded mode. They can work in both modes depending on certain factors, including the operational cost. Hybrid distributed generation systems are generators with energy storage systems that are integrated with the load. These distributed generators can be wind generators, PV power generators, thermal power generators, or conventional generators. Furthermore, a number of storage systems exist, and among these, the most common storage system is the battery storage system. Additionally, flywheel storage and super capacitor systems exist. Energy storage systems have three main objectives: they should smooth the fluctuations in the power output, substitute for any power shortage from the distributed generators (DG), and provide the initial power in the transition between grid operation and islanded operation. DG systems tend to have a low capacity-to-load ratio. DG systems are intended to aid the load side rather than the utility side. The IEEE standard P1547.4 is an important guide on how to design a DG system, operate it and integrate it

with the electric grid, [1]. This standard is, in effect, an improved version of IEEE standard 1547-2003 [2].

1.2 Motivation

Over the past century, radial systems have been used extensively. Only recently have researchers moved towards new system configurations. Two distinct reasons behind the trend towards the new configurations can be observed. An essential reason is simply the desire to increase the reliability of electrical networks. For this reason, researchers have invested effort and exploration into what are referred to as smart grids. Smart grids can be defined in a multitude of ways. For instance, a consumer would define a smart grid as a grid that uses smart wattmeters in his/her home or facility. Indeed, it also denotes having smart or self-controlled appliances. From a utilitarian perspective, smart grids are those that have distributed generation, smart monitoring over the system, and other aspects such as load management and self-healing.

Accordingly, the main target of this work will be to design a hybrid distributed generation system (HDGS) that includes a PV system, a wind turbine, storage, and a diesel generator. Firstly, each system will be designed separately. Secondly, all of those aforementioned subsystems will be combined to form the HDGS. Several factors will be considered to study the effect of this HDGS on an electrical network. Subsequently, the availability of

the diesel generator will be evaluated. The availability of the PV and wind sources will also be studied. In addition, the charging and discharging of the energy-storing units will be included.

1.3 Objectives

A system with smart restoration/self-healing has been an essential goal since the high penetration of renewable energy sources into electrical grids. The aims of this work are assigned as follows:

1. Modelling the conventional distributed generator (DG), PV DG, wind DG, and energy storage systems. The availability of each subsystem will be evaluated based on the ability to supply the load at every hour over the study period.
2. Combining all the subsystems into one HDGS, which will be the complete proposed HDGS model.
3. The complete HDGS will be used as one system and implemented into the microgrid to assess the smart self-healing effect of the HDGS on the microgrid.

1.4 Thesis Organization

This thesis will follow an ordered sequence that is explained as follows. In chapter 2, a literature review will be compiled and presented on the fields of smart grids, micro-grids, distributed generation, renewable sources, energy storage, conventional generators, cost analysis, forecasting and simulation techniques, etc. In chapter 3, the problem shall be formulated by first presenting the hybrid distributed generation system (HDGS) on the one hand and the operational model on the other as well as the equations that relate the inputs and outputs of every subsystem. Subsequently, the physical model of each system will be given and studied from a reliability point of view.

The system will be used in different case studies presented in chapter 4. In the first case study, the HDGS will be allowed to supply only the local load at a load point. In the second case study, the HDGS will be allowed to supply a neighbour load with whatever excess energy it possesses after fully supplying the first load. In the final case study, the HDGS will be given a priority list, based upon which it will supply two loads in order. The simulation results will be presented, and then two cases will be evaluated to study the effect of changing various essential parameters of the system. In each case, one parameter will be changed at a time. Chapter 5 will review the work performed and draw conclusions as well as discuss possible future work that can be conducted.

CHAPTER 2

LITERATURE REVIEW

Renewable energy sources do not require fuel; they are green sources and are very attractive as distributed generators. Thus, for cases when the continuity of power supply is important, as in a hospital, for example, the use of DG sources would be important. However, in most of the world, the use of renewable energy sources as backup generators is still fairly uncommon. This is due to the random intermittency that occurs with renewable energy sources, and for this reason, a conventional generator is used in such cases. However, the combination of renewable energy sources and a conventional DG can provide a more reliable system with fewer environmental effects. To make the renewable energy sources more reliable and able to provide steady power output, energy storage units can be used. This requires a more sophisticated study of the systems, but it will eventually result in better and more reliable systems.

2.1 Distributed Generation

In [3], the authors model a wind distributed generator, and three models were used. The first is made for a non-intermittent DG source. The second model considers the uncertainty in the wind generation and is based on Markov models. Monte Carlo simulation was also

used in the process to model the failure and repair rates of the proposed system. In their third model, the authors simply combined some characteristics of the first model and some of the second. The authors suggested the use of statistical grouping techniques, or what is called clustering, to reduce the number of states. Various DG models were presented in [4], and they were evaluated based upon specific constraints of reliability and economic efficiency. The study also used what is called the fuzzy judgement matrix to help evaluate the reliability of the DGs.

In distributed generation, storage sizing is an important aspect of the design. In [5], the Markov modelling used real metrological data of solar radiation to best size the storage used at the load points. Three main models were presented, and in the first, the storage was simply chosen to be equal to that needed for the days when the load is more than the generation. In the second model, the generation on the days where the load is more than the generation was considered for better results. The final model divided the solar radiation into many states, giving the best results in terms of sizing the storage units. Sometimes, the designer is interested in the power production estimation, as with the case in [6]. To achieve this, reliability indices, such as LOLE, LOEE, and LOLF, were used. The design was completed in MATLAB based on Markov modelling. The model used clustering and Monte Carlo simulation. The authors ~~actually~~ used the reliability modelling to estimate the power production as the final goal rather than the reliability itself.

2.2 The PV System

In [7], the solar radiation was divided into different states by Markov modelling. The aim was to optimize the storage size. In this study, the Markov model incorporated only two states for the solar radiation, but the battery levels were divided into additional states. Furthermore, the battery states were increased to determine the effect of having finer state divisions. A combination of only PV and wind systems was evaluated in [8]. The authors aimed to evaluate the performance of such a hybrid system. In [9], a case study described the voltage levels in some networks in the UK. The issue was the low voltage level in those lines, and the authors used Monte Carlo simulation to evaluate and study this problem. Eventually, they attributed the issue to the length of those lines. In other studies, such as [10], probabilistic methods were used to optimize the design of the PV system. This study used more than just one method. One of the methods used in the study was Markov chain modelling. A battery model allows transitions from a state to neighbouring states only, and it can allow the transitions to go even beyond the neighbouring states. In other words, if there are five states representing the battery, and state one is the totally discharged battery state, there are two ways to model the transitions between these five states. In method one, the transition can, for example, only go from state three to state two or state four, and it cannot go to any state beyond those two neighbouring states. In method two, state three can directly transition to any state; it does not have to be a neighbouring state. A battery model in which the state transition was allowed to pass multiple states was presented in [11].

In [12], a review on experimental microgrids and test systems was performed. The study discussed many topologies used in different places around the world to connect the DG. Some of those topologies also included transformers after the PV or wind systems. A number of systems had more than one PV system, and each one had a different method of placement. A method to test the PV modules' reliability was presented in [13], and in [14], a PV system's reliability effect on a network was evaluated by modelling a PV system and installing it on the IEEE reliability test system. System adequacy indices were used to demonstrate the effect of the PV system used, and the PV system was proved to improve the reliability of the network. A PV system design was shown in [15], and the system was then tested and compared to other representations. Mechanical failure and repair rates of PV strings were given in [16]. Those rates can be used for the physical representation of PV strings that are represented by only up and down states.

The weather effects play an important role in the representation of renewable energy systems. For this reason, in [17], the weather effects were included in the study of the modelling of PV systems. Inverters were then introduced as state models in [18]. This study was not content with simply modelling the inverter and also studied its effect on the reliability of the system. It was observed that, even though the DG systems may increase the reliability of a network, the inverter's failure and repair rates can significantly affect that. Weather statistical data were obtained and used in [19] to model a wind-PV energy

system. The system was broken into states, and these states were numerous for the analysis. To reduce the time required for analysis, the number of states was reduced by the use of fuzzy C-means clustering. The systems were then made into a Markov chain representation. Finally, the systems were added to the Roy Billinton Test System (RBTS) for evaluation. The reliability of the physical components of a wind turbine system were also provided in that study.

2.3 The Wind Turbine Generator (WTG)

The wind speed was recorded at specific locations in Egypt that are appropriate locations to host wind generators [20]. The data were further processed in MATLAB and Simulink. The study considered the wind turbine generator (WTG) as a separate component. Eventually, the system ended up with three composite states. For the wind speed modelling, a Weibull distribution was used. In [21], a simplified model was used to represent the WTG. Most of the focus was on the process of the data, for instance, the wind speed and power output of the WTG. For the case study, the real-life system parameters were taken from the Jeju Island power system in Korea.

In [22], a model for large wind farms was presented. The model did not divide the states based upon the generating units but instead based upon their level of generated power. The transitions were obtained by acquiring the frequency of occurrence and the duration of each

state. The seasonal data were considered to show the effect of the seasons on the reliability of the model. A different way of considering the sizing of renewable DGs was presented in [23]. The analysis was based on the cost considering the interest rate and present worth value concepts.

The reliability of WTGs was considered in [24] by first processing the wind speed data and obtaining the power output of the WTGs. Then, they were divided into states, and the model was simplified by reduction of the number of states. For the RBTS bus-2 system that is used in many studies as a reliability test system, those data were given in [25] and [26]. The failure rate, rating, and specification of each component of the system were provided in [25], [26]. All of the aforementioned work either focuses on one subsystem, such as the wind or PV system, or uses one simulation technique.

2.4 Data Forecast Techniques and Simulations

Because the renewable sources might not be available all the time and their availability cannot be known, historical data can be used to predict them. There are different ways to use the historical data to predict the future results, such as the auto regressive moving average method (ARMA) [27], [28]. By further evaluating the wind speed or solar radiation, the expected power output can be determined [29].

In [30], a PV system was installed in the IEEE reliability test system. The effect of installing the PV system on the reliability indices was investigated. The insertion of a PV system into the IEEE reliability test system improved the reliability indices. In [31], different representations of PV systems were compared. The authors presented a reduced model for the PV system and compared it to other representations. The weather effect on PV systems was included in [32]. As the number of factors increases, both the system's accuracy and complexity increase.

Depending on the technique desired for forecasting the wind speed and the solar radiation, a model has to be created. In [34]-[36], a sequential Monte Carlo simulation was used to simulate the hourly wind speed for a year. In [37],[38], the basic concept of the ARMA method is explained, and the process of choosing the best number of Auto Regressive (AR) and Moving Average (MA) terms is also explained. The ARMA model created can then be used to simulate the wind speed as shown in the aforementioned studies. It is explained in [46]-[47] how to carry out a Monte Carlo simulation for exponentially distributed failure and repair rates. The Auto Regressive Moving Average (ARMA) technique is also useful for such simulations.

2.5 Smart Grids

In this section, smart grids will be reviewed. Smart grids usually include more than one type of generation. Smart grids, as previously stated, can be considered from different views. They are networks that have smart monitoring and energy systems [48]-[50]. Moreover, they have bidirectional power flow and are rather more complex than conventional networks [49]. Thus, reliability studies as well as the design of these smart systems are also rather complex [51]-[52]. Reliability is an important aspect in electrical networks. When reliability is discussed, simply and primarily, it points to the ability to keep power flowing to customers with no or a minimum number of interruptions [53]. Because the reliability of electrical networks is important for both customers and the utility itself, researchers need to invest more work in this direction [48], [54]-[56].

In [57], smart grids are defined as small voltage distribution networks that transfer power to small loads. The essential aspects of a smart grid are the bidirectional power flow, self-restoration/healing, and use of renewable distributed energy sources, such as PV sources [58]. The economic benefits as well as the operational and environmental advantages of using smart grids have been researched in some previously published studies [59]-[63]. In [54], [64], and [65], the effect of using smart grids on the reliability indices of the electrical networks was studied.

2.6 Reliability of Microgrids

Primarily, microgrids have an effect on the system after the occurrence of natural disasters. This issue was addressed and studied in [66]. In that work, Markov state space models were used but were based on the minimal cut sets. This was applied so that the analysis of the problem would be more straightforward. The authors verified their results by comparing them to Monte Carlo simulation results. Regarding the storage system presented in [66], the battery was allowed to move from one state to any other. However, their battery system was slightly modified at some specific points. The reliability and optimal sizing of a standalone PV system was considered in [67]. The analysis was based on a Markov model representation but used the loss of load probability (LOLP) as the design criterion. Fault tree analysis (FTA) and reliability block diagrams (RBD) served the design of their system. The authors tried to avoid Monte Carlo simulation because of the computational time it may require. The design modelled the PV as if it was a string of a number of PV modules. The storage system was also considered as a group of batteries. The main concern of this study regarded sizing the system based upon the LOLP.

CHAPTER 3

PROBLEM FORMULTION AND INPUT DATA

3.1 Modelling the Renewable Resources

Renewable resources are far more complicated than the conventional generator model. Simulations will be needed to represent those systems and their operation. Metrological data can also be used as inputs, whilst the PV system will be divided into two sections – the physical components model and the data simulation model. Those two models can then be put in series. They will be considered in series because the PV system will be considered to be down if it fails physically or if it receives no solar radiation. The physical model will have the PV strings, and the simplest way to represent that is by a two-state model. However, the representation that will be used here will take into account that those strings can work in parallel or in series. Thus, the physical model can have more than two states. The data-based model will have the solar radiation as an input, and this will present a factor of uncertainty that can be accounted for through a Monte Carlo simulation. The output of this PV system will, of course, be its solar power (PS).

3.1.1 The Operational Model of the PV System

The PV system is presented in Figure 3-1. The presented system shows the inputs and outputs of the PV system as well. However, these inputs and outputs are solely for the PV system and form an integral part of the complete HDGS.

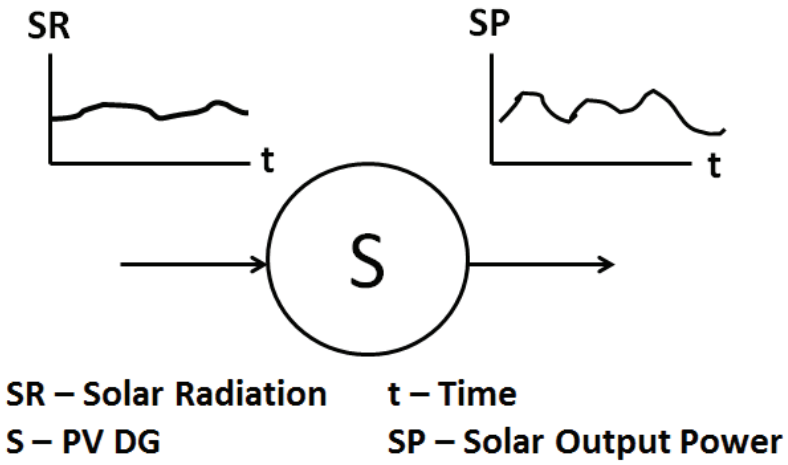

Figure 3-1 The Operational Model of the PV System

The previously mentioned systems can be combined in different ways. They can be converted into Markov states and then analysed. Nevertheless, these systems are better when combined and then converted to Markov states. This is why Figure 3-1 is based on data analysis. For the purpose of considering the uncertainty in the random power generation of solar radiation, a Monte Carlo simulation might be used with an uncertainty

factor to generate solar radiation data for a number of years. The basic equations governing the PV system are [23]:

$$I = I_{sc}\left[1 - exp\left(\frac{V - V_{oc} + IR_s}{V_t}\right)\right] \quad (3\text{-}1)$$

$$Rs = \frac{V_{oc}^* - V_M^* + V_t 1n\left(1 - \frac{I_M^*}{I_{sc}^*}\right)}{I_M^*} \quad (3\text{-}2)$$

where:

I_{sc} - Short-circuit current

V_{oc}- Open-circuit voltage

Rs - Series resistance

Vt - Thermal voltage

$$I_{sc} = I_{sc*}^* \frac{G}{G^*}\left[1 + \frac{dI_{sc}}{dT_c}(Tc - Tc^*)\right] \quad (3\text{-}3)$$

$$Tc = Ta + C_1 Geff \quad (3\text{-}4)$$

$$C_1 = \frac{NOCT(°c) - 20}{800W/m^2} \tag{3-5}$$

$$V_{oc} = \left[V_{oc}^* + \frac{dV_{oc}}{dT_c}(T_c - T_c^*)\right]\left[1 + \sigma_{oc} 1n\left(\frac{Geff}{G_{oc}}\right) 1n\left(\frac{Geff}{G^*}\right)\right] \tag{3-6}$$

where the equation parameters are:

NOCT = normal operating cell temperature of the module

STC = standard test conditions of the module

Isc* = Short circuit current of the module at STC

Voc* = Open-circuit voltage of the module at STC

I_M * = Maximum current of the module at STC

V_M* = Maximum voltage of the module at STC

G* = Irradiance at STC

Tc* = Temperature of the module at STC

Ta = Ambient temperature

Tc = Operating temperature of the module above ambient

Geff = Effective irradiance, related to the incidence angle

dIsc/dTc = Temperature coefficient of the current

dVoc/dTc=Temperature coefficient of the voltage

σoc =Empirically adjusted parameter = ~.04

G_{oc}=Empirically adjusted parameter = G*

$$PV(t) = Npv.Vm(t).Im(t) \tag{3-7}$$

where PV(t) is the power generated, Npv is the number of modules, Vm(t) is the maximum voltage, and Im(t) is the maximum current of the module at time t. For simplicity, if the open-circuit voltage and short-circuit current are directly provided, the following equations can be used [41]:

$$T_C = T_A + \frac{s(NOCT - 20)}{.8} \tag{3-8}$$

$$I = s[I_{SC} + K_I (T_C - 25)] \tag{3-9}$$

$$V = V_{OC} - K_V T_C \tag{3-10}$$

$$FF = (V_{MPP}\, I_{MPP})/(V_{OC}\ \ I_{SC}) \tag{3-11}$$

$$P_{PV} = N * FF * V * I \tag{3-12}$$

where T_C is the temperature of the cell (in Celsius), I is the short-circuit current of a PV cell (in amperes), K_I is the temperature factor of the short-circuit current (in amperes / Celsius), V is the open-circuit voltage (in volts), and K_V is the open-circuit voltage temperature factor (in volts / Celsius). FF refers to the fill factor. V_{MPP} and I_{MPP} are the voltage and current at maximum power under normal operating conditions, respectively. V_{OC} and I_{SC} are the open-circuit voltage and current, respectively. The solar radiation level is denoted by 's' in the equations above.

3.1.2 The Operational Model of the WTG

In the same manner, the wind system also has its own separate design. The idea does not vary much from that of the PV system except that the equations processing the inputs are different. However, the scheme used to process the data of each system can be different for many purposes, one of which is the comparison. Figure 3-2 shows the separate system of the wind turbine generators.

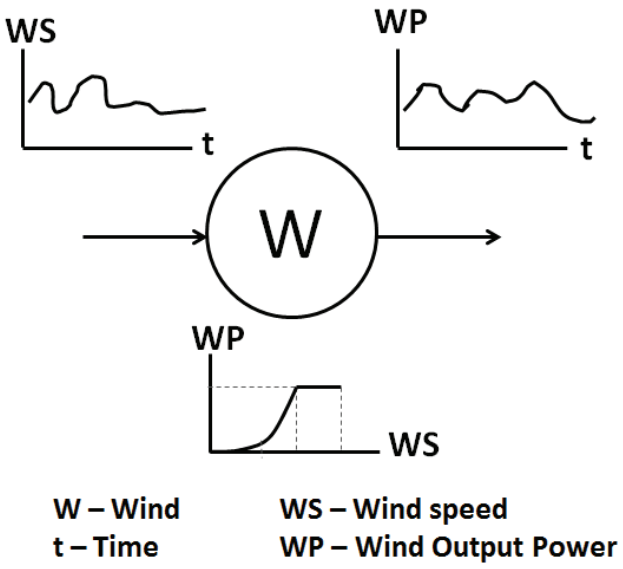

Figure 3-2 The Operational Model of the Wind System

Figure 3-2 shows that the wind speed data has to be retrieved by means of a Monte Carlo simulation, and the data are processed based upon the turbine's power output vs. wind speed curve. This will result in a power output curve that can be combined with the output of the other systems to make the HDGS. The wind system basically follows the set of equations below [21]:

$$P = \frac{1}{2} c_p p V^3 A \tag{3-13}$$

where:

P – Theoretical Power [W].

Cp - Power coefficient.

p - Air density (1.225 kg/m^3).

V - Wind velocity (m/sec).

A - Swept area of the rotor disc (m^2).

$$Pi = \begin{cases} 0, & 0 \le SWi < Vci \\ P_R(A + B \times SWi + C \times SWi^2), & Vci \le SWi < V_R \\ P_R, & V_R \le SWi \le Vco \\ 0, & Vco < SWi \end{cases} \quad (3\text{-}14)$$

The parameters A, B and C are given by:

$$A = \frac{1}{(V_{ci} - V_R)^2}\left[V_{ci}(V_{ci} + V_R) - 4(V_{ci}V_R)\left(\frac{V_{ci} + V_R}{2V_R}\right)^3\right] \quad (3\text{-}15)$$

$$B = \frac{1}{(V_{ci} - V_R)^2}\left[4(V_{ci} + V_R)\left(\frac{V_{ci} + V_R}{2V_R}\right)^3 - (3V_{ci} + V_R)\right] \quad (3\text{-}16)$$

$$C = \frac{1}{(V_{ci} - V_R)^2}\left[2 - 4\left(\frac{V_{ci} + V_R}{2V_R}\right)^3\right] \quad (3\text{-}17)$$

where:

SWi – Wind Speed at the ith hour [m/s].

Pr – Rated power [W].

Vr – Rated speed (m/s).

Vci – Cut in speed (m/s).

Vco - Cut out speed (m/s).

3.2 The Model of the Conventional DG

The conventional generator will be represented by a two-state model. These two states are either up or down. This model does not need to be more complex, as its power output is steadier than that of the renewable resources. The price signal can be added at a later stage as an input signal to the model of the conventional DG. Thus, the input to this system can be the price signal, and the output will of course be the power output of the conventional DG (PDG). The price of electricity is what is meant by the price signal here.

The conventional DG is not a random power generator, as is the case with the renewable sources. Thus, its model will not be dependent on factors such as PV radiation and wind speed. The fuel source can be assumed to be 100% reliable. In this study, the conventional DG would be considered with an input, and this input would be the price signal. In other words, when the electricity generated by other sources is expensive, the DG can work instead, and vice versa. Figure 3-3 shows the operational design of the conventional DG.

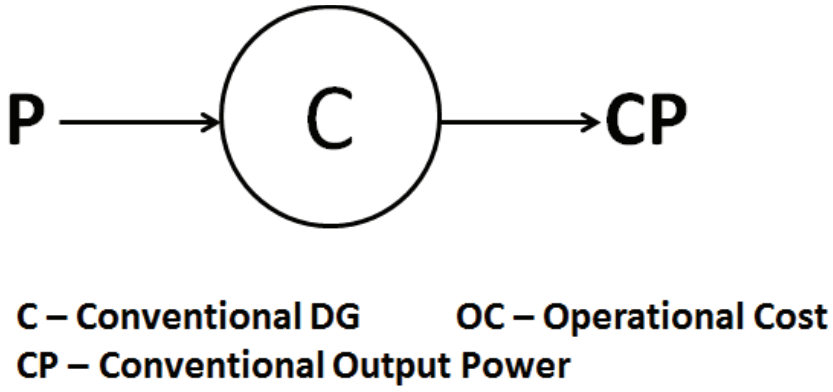

Figure 3-3 The Operational Model of the Conventional System

The conventional DG will give power output that is still not difficult to combine with the output of the other sources. After that, the final output can be sent to the battery or the microgrid.

3.3 The Model of the Energy Storage System

The energy storage system will be the one to store the excess energy from the renewable sources. It will also act as a backup source. Additionally, the storage system makes up for the fluctuations in the output of the renewable sources. Figure 3-4 shows the operational diagram of the storage system and its interaction with the rest of the system.

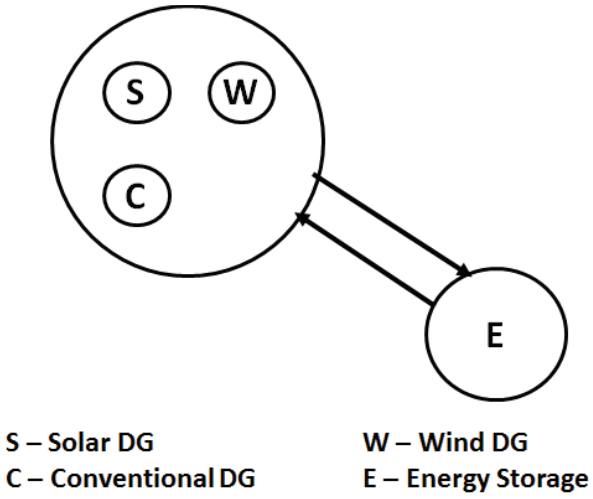

Figure 3-4 The Operational Model of the Storage System

The battery is not governed by power generating equations but rather by a charge and discharge process. Thus, it can be implemented with the other components of the system after they have all been combined together. Subsequently, the full HDGS would be installed on a load point with failure and repair rates. The flowchart that governs the process of interaction between the PV system and the storage system is shown in Figure 3-5. The same process exactly applies to the case between the wind system and the storage system. It is important to note that the battery system is common to the wind and the PV systems, and thus, merging the two processes will be considered. Points ‘B’ and ‘C’ on the flowchart are the points at which the diesel generator will be inserted. The flowchart of the diesel generator is shown in Figure 3-6, and it will be inserted at points ‘B’ and ‘C’ as mentioned.

In the following flowchart, the power generated by the renewable sources will serve the load. If the power generated by the renewable sources is insufficient, the battery will be discharged to feed the unfed load. If the battery and the renewable sources are not enough to supply the load, the diesel generator will be operated. Any excess energy from the renewable sources will be used to charge the battery under the condition that the battery is not fully charged yet. All the parameters used in Figure 3-5 and Figure 3-6 are explained in Table 3-1.

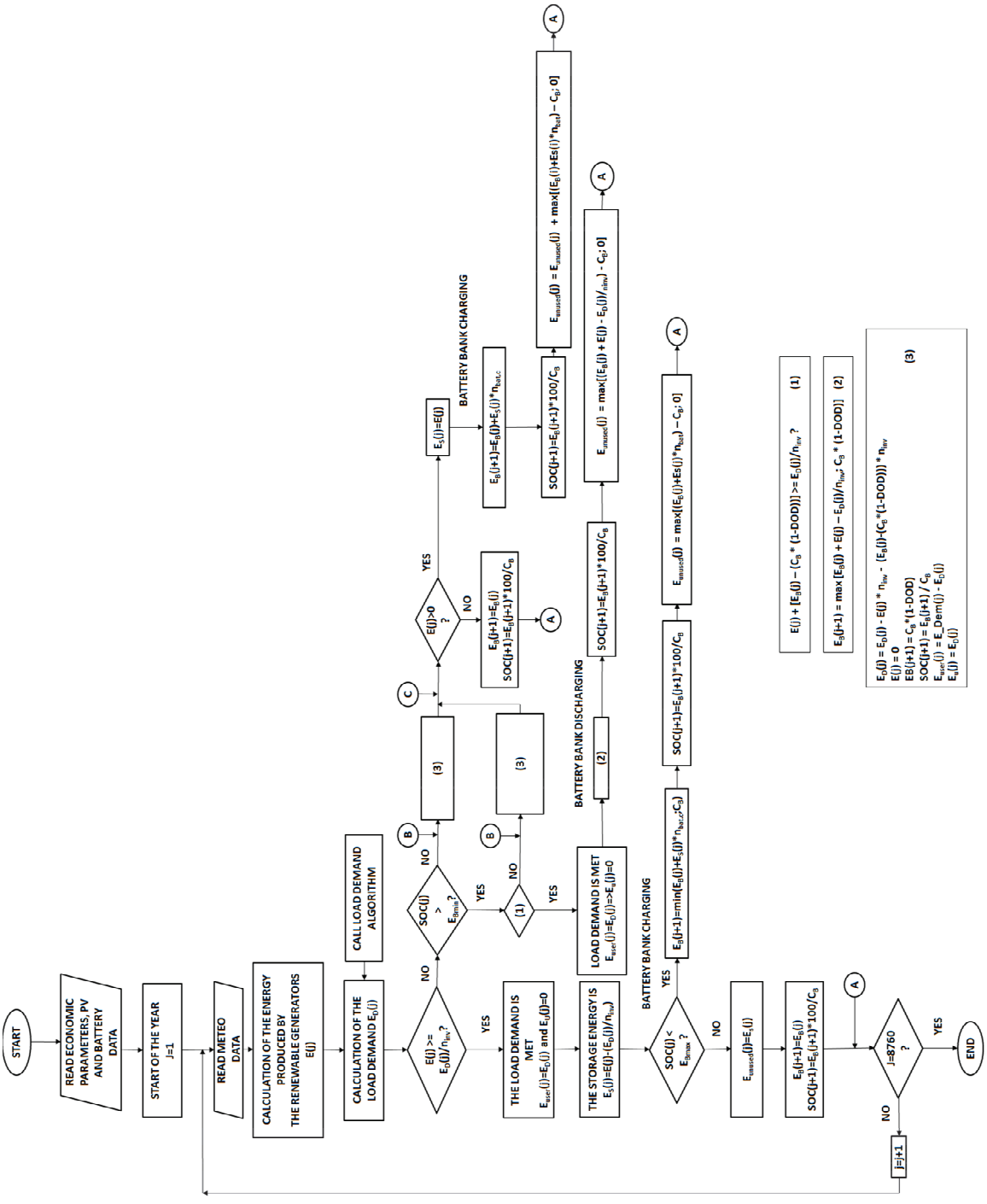

Figure 3-5 Flowchart of the Flow of Energy

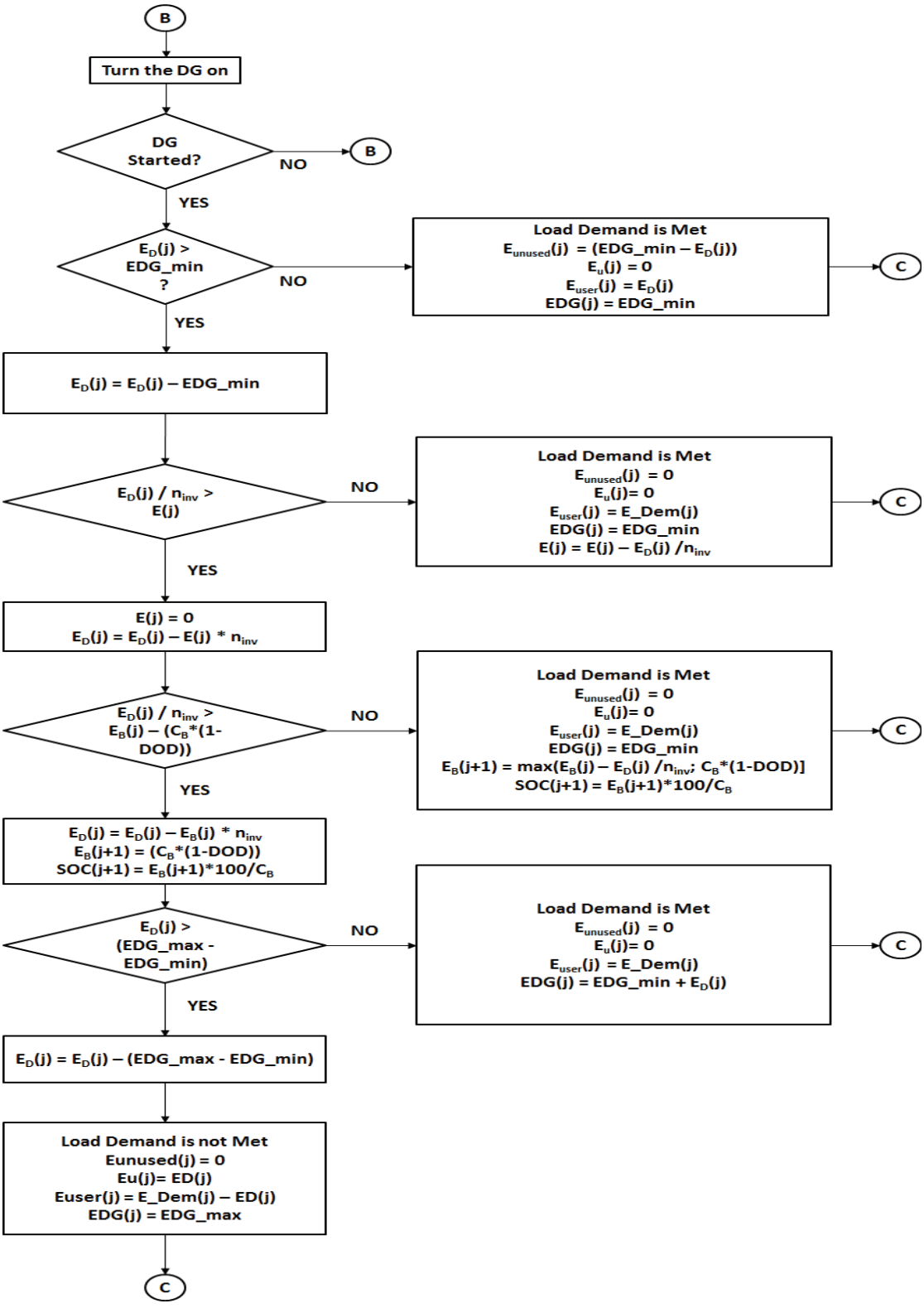

Figure 3-6 Diesel Generator's Energy Flow Incorporation into The System

For the variables shown in Figure 3-5, all the variables are declared in Table 3-1. The efficiencies and other parameters mentioned in the flowchart are recorded in Table A-1.

Table 3-1 Variable Definitions

Variable	Definition
DOD	Depth of discharge
E	Energy
j	Hour of the year
SOC(j)	State of charge at jth hour
ηbat	Battery efficiency
ηinv	Inverter efficiency
CB	Battery capacity
E_Dem	The energy demand
E_D	A temporary variable of energy demand
E_DG_min	The maximum energy generated by the diesel generator
E_DG_max	The minimum energy generated by the diesel generator
Subscripts	
B	Available battery bank energy
Bmin	Minimum battery charge
Bmax	Maximum battery charge
D	Energy load demand
PV	Energy produced from the PV generator
S	Energy for storage
U	Unsatisfied energy
User	Energy supplied to the user
Unused	Unused energy (full battery)

3.4 The Operational Model of the HDGS

Firstly, the HDGS is divided into subsystems, and each is made of different components. The HDGS will be composed of four main components that will later be connected to the grid. The storage model will be represented as a system of batteries that will have states of charge (SOC). The charging and discharging rates will be based on generation. The storage system will be common to all the DG sources. The transitions between the SOC of the battery can be allowed to move multiple states in one transition, i.e., to non-neighbouring states, or they can be restricted to move to the neighbouring states only. The number of SOC can be large for finer results, but that would be to the detriment of the simulation time, and thus, the number of states can be reduced by means of clustering.

Several studies in the literature discuss how to design a PV DG, how to size it, and its effect on the system. Typically, only one of those aspects is addressed at a time. The wind system is similar in overall design to the PV system. These two systems suffer from the problem of random power generation, or more precisely, intermittent power generation. For this reason, an energy storage system is usually combined with those two systems in regard to either designing the system or studying its reliability. For the conventional/diesel DG, reliability is not heavily invested for a separate DG because it tends to function as a backup source or is combined with renewable DGs. In other words, the conventional DG is usually studied with other subsystems rather than being studied separately.

In this work, all the components will be combined in what will be called the hybrid distributed generation system (HDGS); see Figure 3-7. This HDGS will assess the network in the case of natural disasters, maintenance of network connected sources, or even when the microgrid is working properly. In case of natural disasters or maintenance, the HDGS will work in an islanded mode, and the need for the HDGS in this case makes sense. If the microgrid is working well, the HDGS can still be used. This could be due to the price difference or other factors.

First, the system needs to be designed on a common ground. Thus, the data will be processed for each system alone, and then all the systems will be combined into one system. Furthermore, the complete HDGS will be presented in terms of Markov chains. It is possible to represent each system by its Markov model and then combine them, but the process of combining the two systems might be more difficult. The operation model of the full system is shown in Figure 3-7.

The wind power generation system will require the wind speed as an input. This can be performed with the Monte Carlo simulation as well. By using the wind speed vs. wind power curve, the power output of the wind system (PW) can then be calculated. PW will be the output of this wind power generation system. It can then be divided into states, and

this can be conducted using the convolution of the power generation and load curves or by other means. The process of dividing the system into states can also be applied to the PV system. It is very important to represent the components by their data, combine the data, and then divide them into states so that the model can be generalized for any data. In case each model is made into states before combining the models, any change of the data will require a change of every model and then a change in the combined models. Both options are valid, but the first one is easier to modify.

Each of the DC power-generating systems requires inverters. Those inverters can be central, i.e., one or a few inverters will connect the complete DC system to the AC one. Alternately, they can be distributed, i.e., each system will have its own inverters. The WTG is composed of physical components that are in series, and its model will involve the physical components inside the wind turbine such as the tower, rotor, and yaw system.

After combining all of the models together, they will be implemented on a utility grid. For this purpose, systems such as the Roy Billinton Test System (RBTS) can be used. Evaluation of the reliability of such systems will be conducted, and this will be followed by two case studies. Finally, the effect of the HDGS on the self-healing of the network can then be assessed.

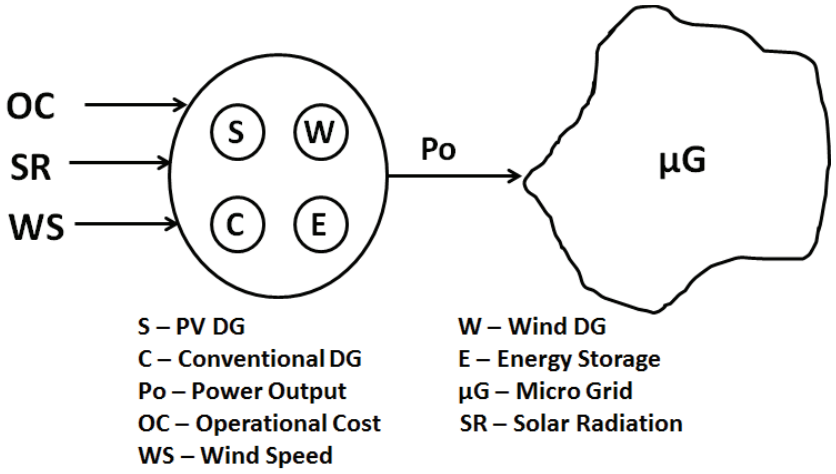

Figure 3-7 The Operational Connection of The HDGS

The HDGS is made of four main components: the PV DG (S), the wind DG (W), the conventional DG (C), and the energy storage system (E). The system takes three main inputs, namely, the operational cost (OC), the solar radiation (SR) and the wind speed (WS). The WS signal will be an input to the wind DG block, the SR signal will be an input to the PV DG block, and the OC signal will be an input to the conventional DG block. All of the systems will naturally provide power as an output, which will be injected into the microgrid (µG). The energy storage saves excess energy from the HDGS, or it can save the energy for later usage. It will also discharge into the microgrid in case the HDGS is not able to fully supply the load by itself.

3.5 Auto Regressive Moving Average Representation

To apply the input/output relationship of a PV or wind system, historical data are needed. This historical data include the wind speed, the ambient temperature and the solar radiation. The data need to be modelled and simulated to account for their unpredictable behaviour. Therefore, the ARMA technique can be used to make a model for the input data, and this model can be used for short- or long-term forecasting. The simulated input data can then be substituted into the input/output equations of the subsystems to obtain the simulated power output.

Usually, the ARMA model is written in the notation ARMA (n, m), where n and m are the numbers of AR and MA terms, respectively. The general format of the ARMA model is as follows:

$$y_t = \emptyset_1 y_{t-1} + \emptyset_2 y_{t-2} + \cdots + \emptyset_n y_{t-n} + \alpha_t - \theta_1 \alpha_{t-1} - \theta_2 \alpha_{t-2} - \cdots - \theta_m \alpha_{t-m} \quad (3\text{-}18)$$

where $\emptyset_i$ (i = 1, 2 . . . . . n) and θ_j (j = 1, 2 . . . . . m) are the AR and the MA parameters of the model, respectively. The normal white noise with zero mean is represented by α_t , and it has a variance of ${\sigma_a}^2$. Thus, by using historical data, the coefficients in the aforementioned equation of the ARMA model can be obtained. The question is how to determine the best number of terms required in the ARMA model. In other words, the ARMA (p, q) model's quality depends on the value of 'p' and 'q' as well. There are several

techniques that can be used for this, one of which is the Akaike or Bayesian information criteria AIC/BIC technique. In this technique, different values of ‘p’ and ‘q’ are tested, and for each case, the ARMA (p, q) model is given an optimized loglikelihood value. This value can then be used to calculate the AIC/BIC. The ARMA (p, q) model that has the lowest value of AIC/BIC is the best model to use for the given data. The AIC/ BIC indices are the ones used in this work.

3.6 Monte Carlo Simulation

All failures and repairs were represented by Monte Carlo simulations. Monte Carlo simulations can be applied to different types of probability distributions by using the inverse transform method. To perform a Monte Carlo simulation for an exponential distribution, the inverse transformation of that distribution must first be obtained, and then the resulting function can be used for simulation. This is explained in detail in the following steps:

1- Obtain the probability distribution function (pdf), f(x), and the cumulative distribution function (cdf), F(x), of the exponential distribution.

$$f(x) = \begin{cases} \lambda\, e^{-\lambda x}, & x \geq 0 \\ 0, & \mathrm{x} < 0 \end{cases} \tag{3-19}$$

$$F(x) = \begin{cases} 1 - e^{-\lambda x}, & x \geq 0 \\ 0, & \mathrm{x} < 0 \end{cases} \tag{3-20}$$

2- Set R = F(x) for the range of x. Note that R is a uniformly distributed number between 0 and 1.

3- Obtain the inverse of the equation.

$$\begin{cases} R = 1 - e^{-\lambda x} \\ 1 - \mathrm{R} = e^{-\lambda x} \\ \ln(1 - \mathrm{R}) = -\lambda x \\ \mathrm{x} = \dfrac{-\ln(1 - \mathrm{R})}{\lambda} = \dfrac{-\ln(\mathrm{R})}{\lambda} \end{cases} \tag{3-21}$$

4- Generate a uniformly distributed number R between 0 and 1 and obtain the value of x. This operation can be performed as many times as needed.

3.7 Cost Analysis for the Subsystems

To calculate the cost, the present worth value, salvage value, operation and maintenance, and fuel cost should all be considered. For generality, the cost analysis will be shown for a PV, wind, and a diesel generator. However, the main focus will be the operational cost of the conventional DG, which is the diesel generator in this case. If all models are considered in the cost analysis, the net present cost (NPC) shall be calculated for all of

them. The main aim will of course be to have a system that works for the minimum cost. Thus, the objective function would be [23]:

$$minimize\ NPC = \sum_{j=1}^{4}[(I_j - S_{dj})X_j + OM_{dj}E_j] \tag{3-22}$$

The term 'j' accounts for the 4 main components of the system (wind, PV, storage, and diesel generator). I_j is the sum of all present capital costs of a unit j. S_{dj} is the salvage value expressed in the present time. The number of generating units is represented by X_j. The present cost of operation and maintenance is denoted as OM_{dj} , while E_j expresses the energy output of the jth unit. The present worth factor (PWF1) is used to obtain the present worth value of a component [23]:

$$PWF1 = \frac{(1+i_r)^N - 1}{i_r * (1+i_r)^N} \tag{3-23}$$

where N is the lifetime of the unit in years and i_r is the annual interest rate. For such a unit, the salvage value in terms of the present worth can be obtained by the multiplication of the salvage value by PWF2 [23]:

$$PWF2 = \frac{(1+i_F)^N}{(1+i_r)^N} \tag{3-24}$$

where i_F is the inflation rate. For a unit that requires replacement, such as the battery or diesel generator, the equations require modification. To calculate the present capital cost for such a unit, the following equation is used [23]:

$$I_j = \ CCU * \sum_{x=1}^{xd} \left[\frac{(1+i_F)}{(1+i_r)}\right]^{(x-1).Ld} \tag{3-25}$$

where CCU is the unit's capital cost, Ld is the unit's lifetime, and xd is the number of units purchased in the project's lifetime. The present cost of the salvage value of such a unit can be obtained by [23]:

$$S_{dj} = \ S_d * R_d * \sum_{x=1}^{xd-1} \left[\frac{(1+i_F)}{(1+i_r)}\right]^{x.Ld} + \ S_{bt} * R_d * \left[\frac{(1+i_F)}{(1+i_r)}\right]^{N} \tag{3-26}$$

$$S_{bt} = \left[\frac{S_d - \alpha_d}{Ld}\ \right] * years + \ \alpha_d \tag{3-27}$$

where S_{bt} is the salvage value of the last unit purchased, S_d is the salvage value of a unit, α_d is the capital cost of a unit, 'years' is the number of years the last unit lasted in the project, Ld was previously explained, and Rd is the unit's capacity. For the OM cost, the OM cost of the battery is set as one cost, but for the case of the conventional DG, this cost will be divided into fuel cost (FC) and maintenance cost (MC) [23].

$$OMG = (MC + FC) * S_{DG} * DG_h * PWF1 \quad (3\text{-}28)$$

$$OMB = K_{OMB} * S_B * PWF1 \quad (3\text{-}29)$$

In the above equations, $S_{DG}, and\ DG_h$ are the size and hours of operation of the conventional DG, respectively. OMG and OMB are the OM costs of the conventional DG and the battery, respectively. S_B is the size of the battery, while the battery is assumed to have a salvage value of 0. The operation and maintenance battery cost is represented by K_{OMB}.

3.8 Physical Modelling of Renewables

In the previous subsections, the operational models and the scheme that will be followed in simulating the data were presented. In this subsection, the physical model will be presented. For the wind system, the design is made of many physical components, while the PV system is based mainly on the modules or strings. For the conventional DG, the operational system can be considered the same as the physical system. This is because the two-state representation of the conventional DG comprises the physical up and down states.

There will be two physical states of the conventional DG, as follows: the working state and the failure state. The physical model of the conventional DG is simply one block of the

generator itself. The PV DG will be made of the PV string as stated and the DC-DC boost in case it is used. The wind and PV DGs will have an inverter at the last stage before being connected to the grid. The physical system of the PV DG is shown in Figure 3-8 and Figure 3-9, while the physical system of the wind DG is shown in Figure **3-10**.

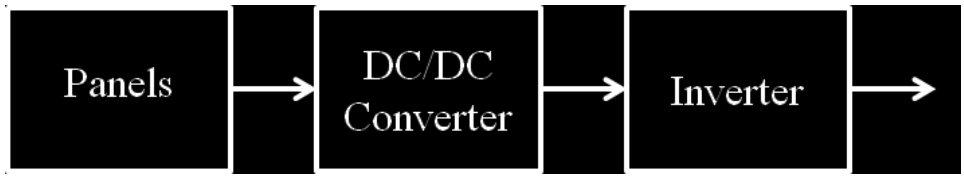

Figure 3-8 The Physical Model of the PV DG

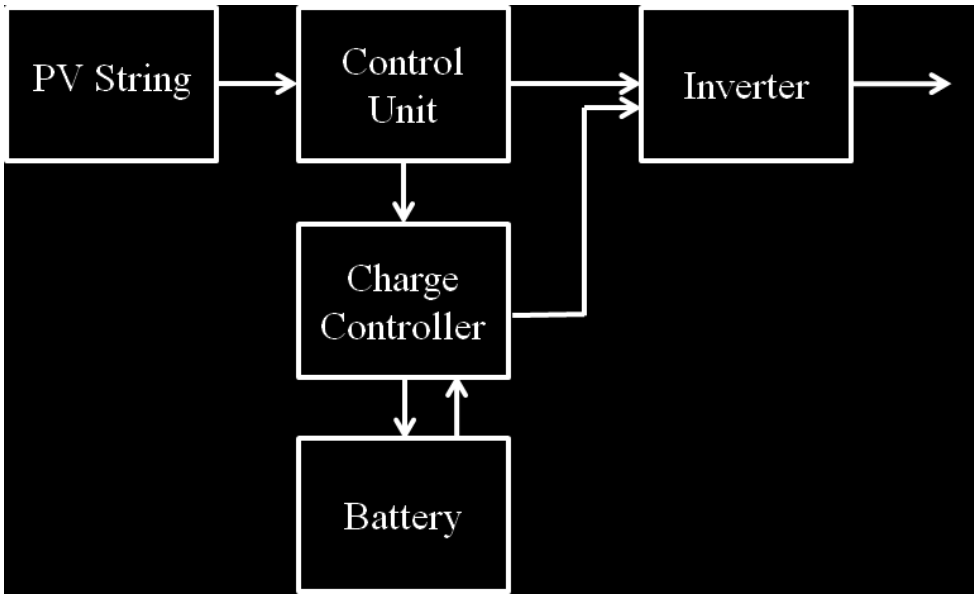

Figure 3-9 An Advanced PV Physical Model

Figure 3-9 shows the PV physical model, but it refers to the PV subsystem as a whole instead of just the PV strings. Those other components are placed in the figure to clarify the connection from the PV system to the load, which will of course come after the inverter stage. The model in Figure 3-9 takes more components into account and thus will be the model used in this work for more accurate results.

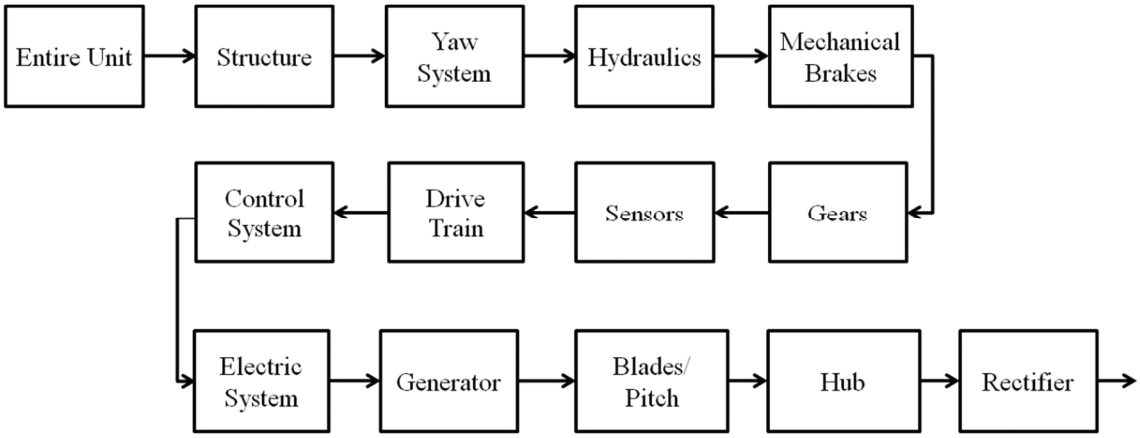

Figure 3-10 The Physical Model of the Wind DG

Figure **3-10** shows a combination of components that are all in series. Those components together form the wind turbine generator (WTG). This WTG can then be connected to the load through the rest of the system's components, as shown in Figure 3-11.

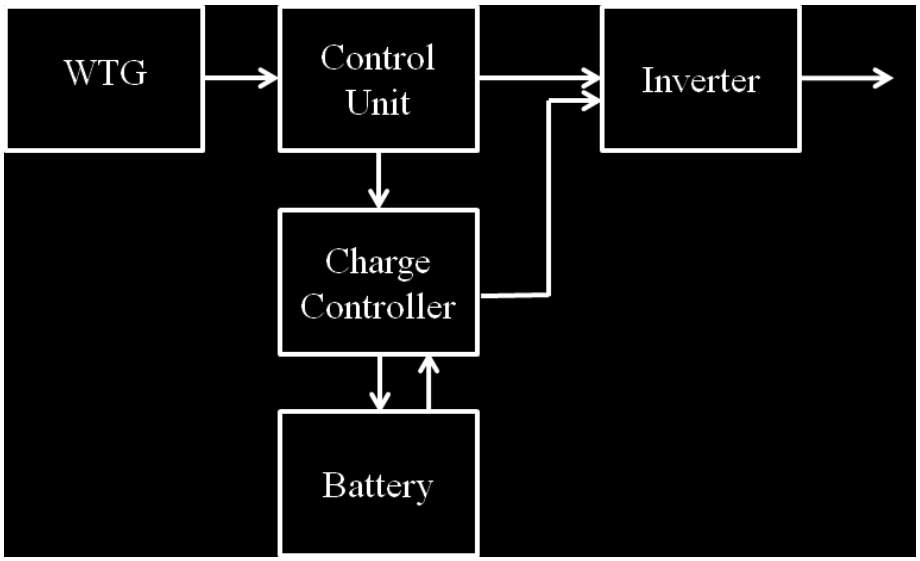

Figure 3-11 Connection from the WTG to the Load

For the diesel generator, control unit, charge controller, WTG, and PV string, the reliability model will be made of two states. The up state is when the system is working properly, and the down state is when the system produces no output.

3.9 Reliability Modelling and Markov States

The reliability modelling will make use of the Markov chain modelling. This part can be perceived in two different ways, as was explained earlier. In the first, the complete system can be combined from an analytical data point of view and then converted into Markov states. This case seems to be easier when combining the systems, and it can be represented as shown in Figure 3-12. In case each subsystem is represented in Markov states alone,

each subsystem will look similar to that shown in Figure 3-12 except for the conventional DG, which will be similar to that shown in Figure 3-13.

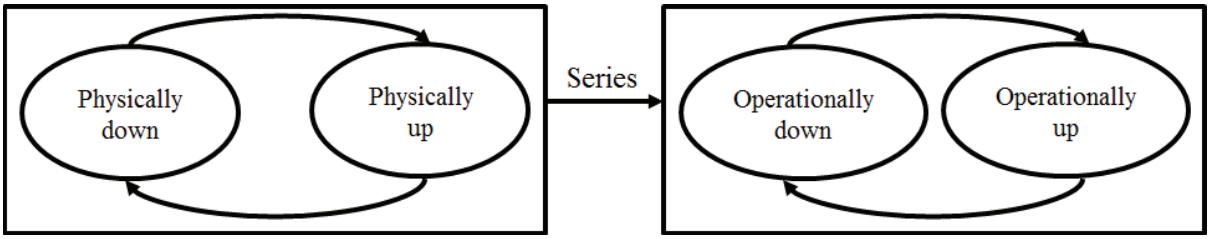

Figure 3-12 The General/Subsystem Reliability Model

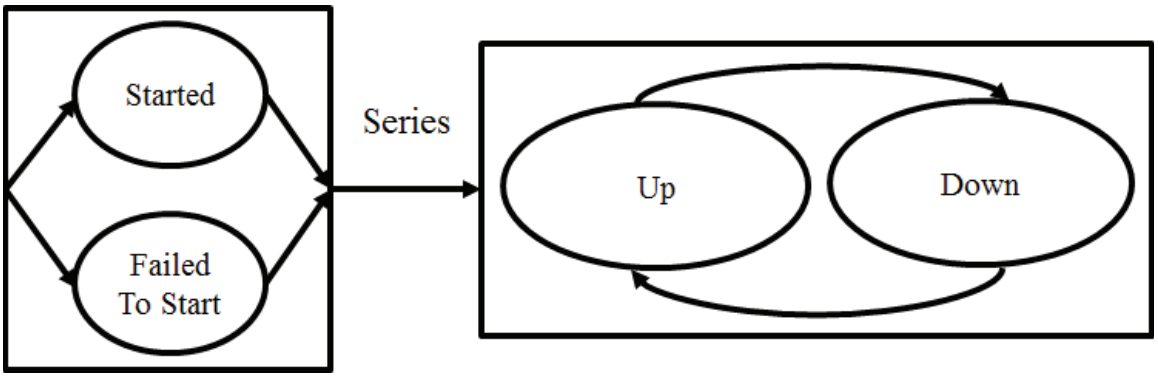

Figure 3-13 The Reliability Model of the Conventional DG

Figure 3-12 is one way to combine the operational and the physical systems. However, this will lead to a system with more states as well as a more complicated scheme. To avoid this scenario, the operational system can be integrated into the battery model. Thus, the battery

can manage the process of the power exchange and work in parallel with the physical model of the WTG, PV, and diesel systems.

From a reliability point of view, if, for example, the PV system is made up of more than one string (which is usually the case), the reliability of those strings can be modelled as shown in Figure 3-14. The figure indicates that, if there are N strings, the failure rate of one of them is N.λm, while λm is the failure rate of just one of them.

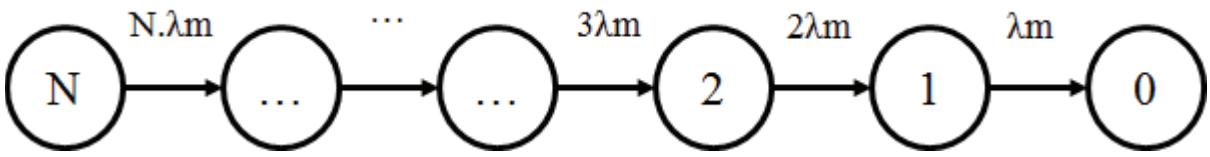

Figure 3-14 Markov model of the PV Strings

The models for the different components of the HDGS have been achieved in the previous sections. In this section, the failure rates, repair times, mean time to failure (MTTF), mean time to repair (MTTR), costs, and any other data used will be listed. In Table A-2, the failure rates and repair times of all of the wind system's physical components are listed [19], [39]-[40].

Table A-3 and Table A-4 show the PV panels, inverter, charge controller, control unit, and WTG rectifier data as well as the systems' costs [19],[67], and [23]. Table A-5 shows the PV system's parameters, while Table A-6 provides the parameters for the wind system [41]. Table A-7 shows the diesel generator's reliability data [41], [68].

The per unit load data were obtained from [42]-[44]. The solar radiation, ambient temperature and wind speed were obtained from [45]. The wind speed, solar power, and ambient temperature from the aforementioned source are for US cities only, and they are divided into three classes. Class I denotes that the data provided has a low error percentage, while class II denotes that the data contains a marginally higher error percentage. A third class that might contain data gaps also exists. The data were obtained for Midland International Airport, Texas, US, and this specific place was selected due to having decent solar radiation and wind speed. In addition, the data were chosen as class I to guarantee the best possible accuracy. The data were not taken for one year but rather over a longer period of time (1991-2005), and for each month, the most accurate data of that month from the entire span of years were taken as an average to represent that specific month. Thus, it is possible that the first month of the year would be from 1991 while the second could be from 1995. However, the 12 months together represent the best average of the required data covering all the years.

3.10 The Comprehensive Model of the HDGS

In the previous sections, a detailed explanation of each subsystem of the HDGS was presented. Each component was separately described, and its data were provided as well as the general idea of how those subsystems will be connected. In this section, the final picture of the complete HDGS will be given. The final scheme for analysing the full system will be discussed, the case studies are described, and the results will be provided. The overall design of the HDGS with all inputs and outputs is shown in Figure 3-15. The WTG block contains the equivalent system of all the components shown in Figure **3-10**. The battery block is common between the renewable systems, and it interacts with them according to the process provided in the flowchart in Figure 3-5.

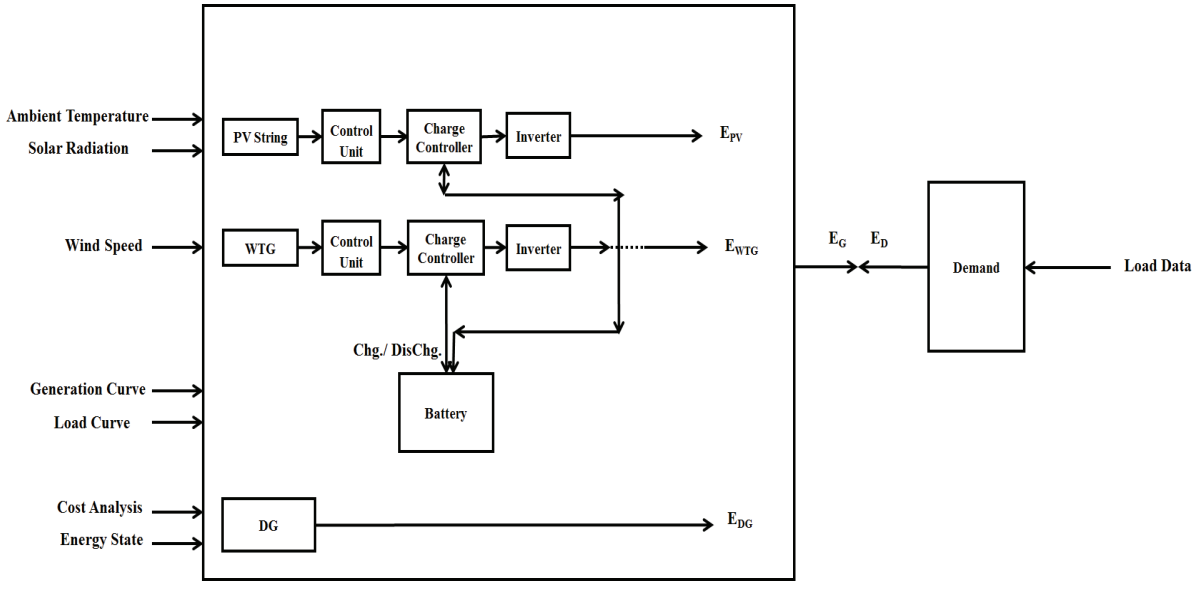

Figure 3-15 The Complete Detailed HDGS

CHAPTER 4

CASE STUDIES AND SIMULATIONS

4.1 The HDGS's Data Forecast

Initially, from a physical point of view, all the blocks in Figure 3-15 are simplified to two state blocks – the fail state and success state. However, the physical model of the battery is not yet provided. In addition, the WTG block consists of many components in series that can be combined into one equivalent component with two states. In Table 4-1, the failure rate and the mean time to repair the battery are shown, which then become represented as a physical component with two states: success or failure. The equivalent rates for the WTG block are also shown in the table [67].

Table 4-1 FINAL FAILURE RATE AND REPAIR TIME [67]

Component	Failure Rate (1/year)	MTTR (h)
Battery	0.1	175.18
WTG	0.403	130.19

To obtain the output power of the PV and wind systems, the ambient temperature (TEMP), solar radiation (SR), and wind speed (WS) of the same location will be provided. The data were obtained for Midland International Airport, Texas, US. The data were obtained and plotted versus time, and then a sequential ARMA short-term forecasting scheme was used to predict the future data for the TEMP, SR, and WS. The forecasted data points are then plotted versus time. However, some data points are unacceptable, for example, those having solar radiation that is less than zero. Such data points will be corrected, and in this case, the data will be set to zero, and the forecasted plots will also be corrected. Therefore, there will be three figures for each set of data. The first will be for the obtained data, the second will be for the forecasted data, and the third will be for the forecasted data after applying corrective modifications. In the following set of figures, the obtained data points will be plotted for the SR, its forecasted data points, and its corrected data points. Next, three similar plots will be shown for the TEMP. For the WS, three figures will be presented in the same order mentioned for the SR and TEMP.

Figure 4-1 shows the yearly average solar radiation (SR) obtained from the metrological data, while Figure 4-2 shows the forecasted solar radiation using the ARMA model.

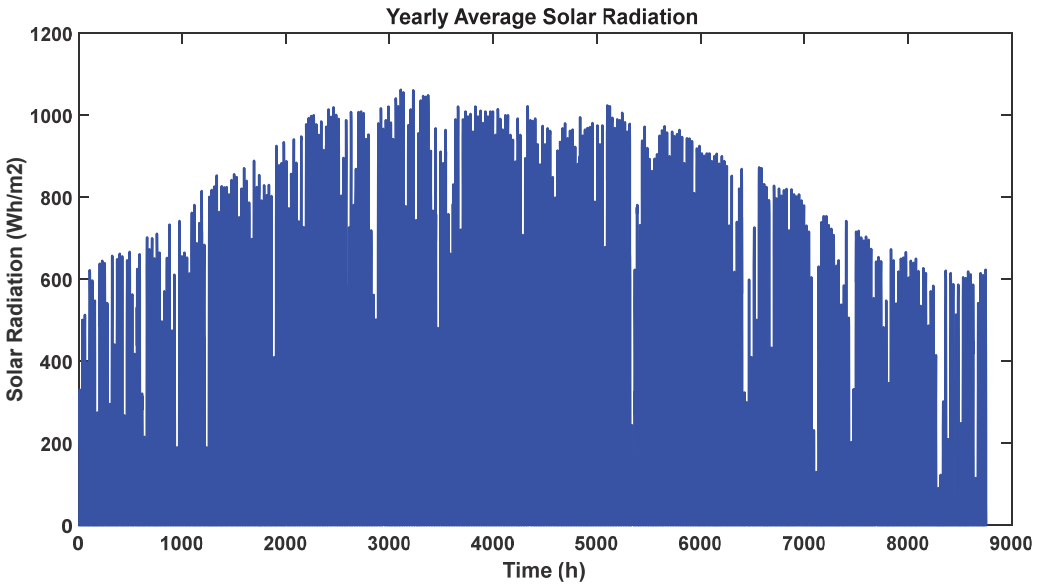

Figure 4-1 Yearly Average Solar Radiation, Metrological

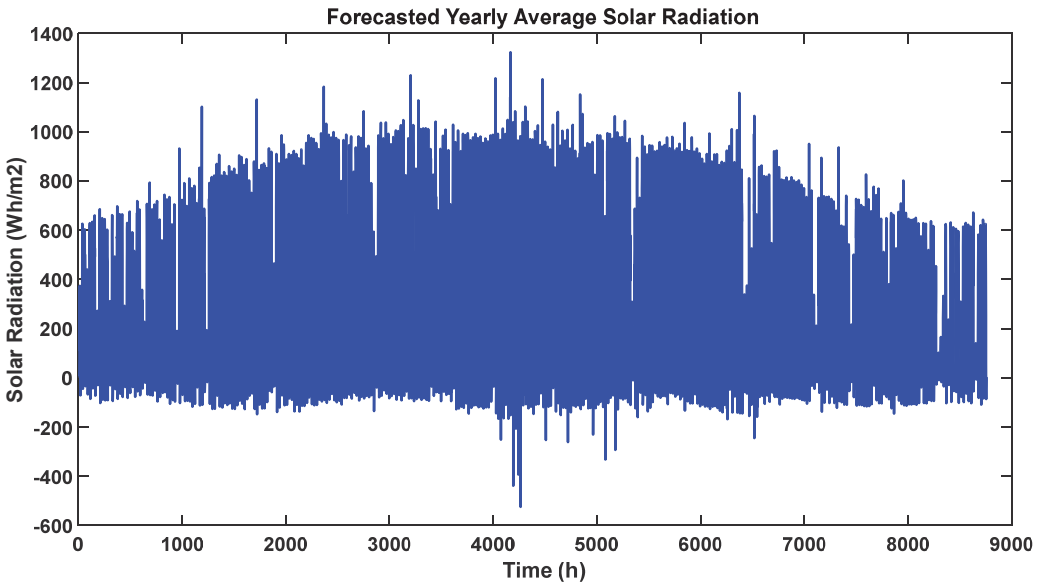

Figure 4-2 Forecasted Yearly Average Solar Radiation

Figure 4-3 presents the forecasted data that has been corrected by eliminating any abnormal points from the data forecast. For example, Figure 4-2 shows that some of the forecasted solar radiation points are below zero, which is not an allowed value. Thus, such values need to be set to zero. This is one type of correction, and the resulting curve after applying the correction is named the corrected solar radiation.

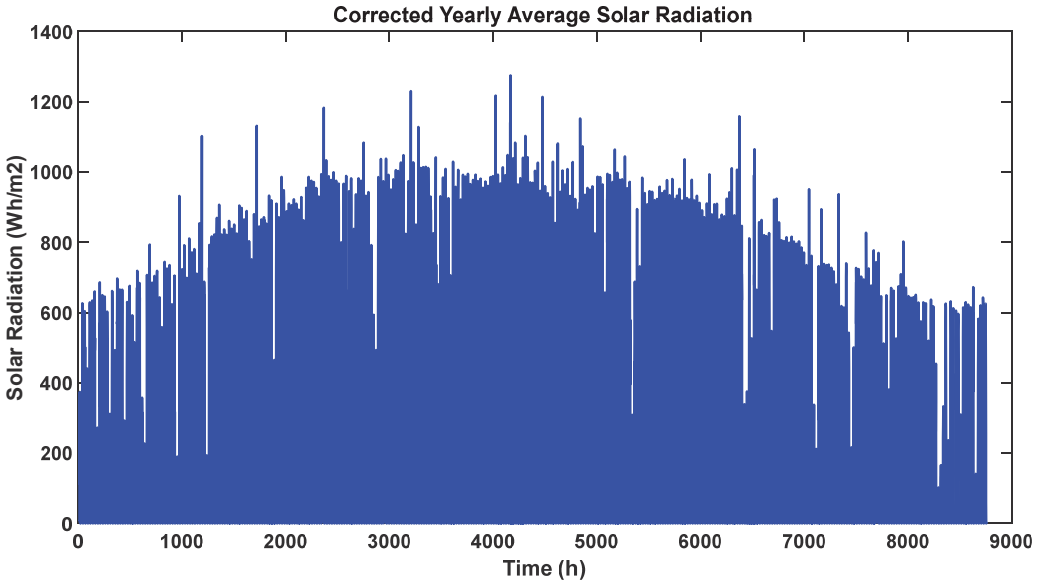

Figure 4-3 Corrected Yearly Average Solar Radiation

Similar to the case of solar radiation, the retrieved ambient temperature (TEMP) is shown in Figure 4-4, and the forecasted data are shown in Figure 4-5.

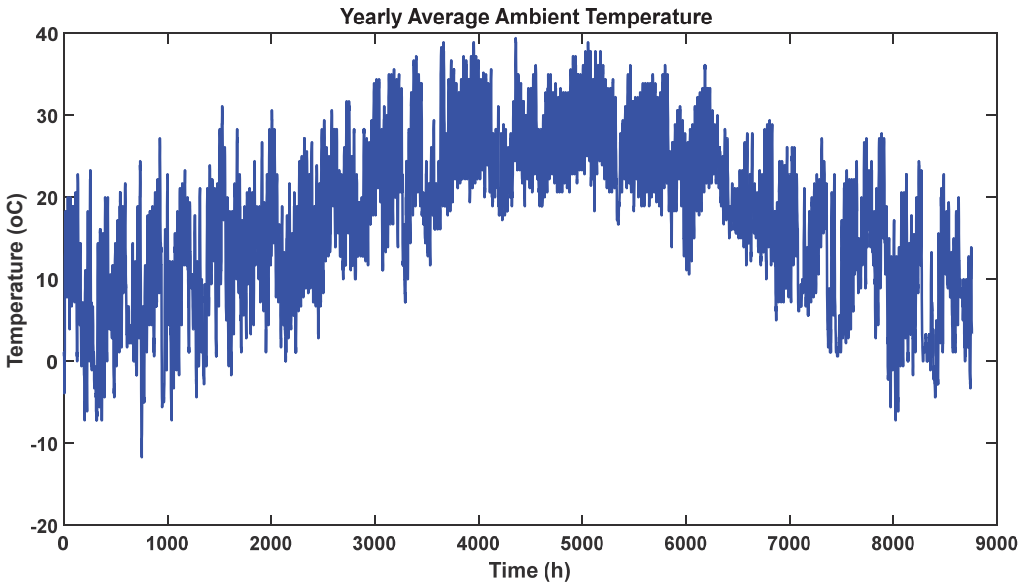

Figure 4-4 Yearly Average Ambient Temperature

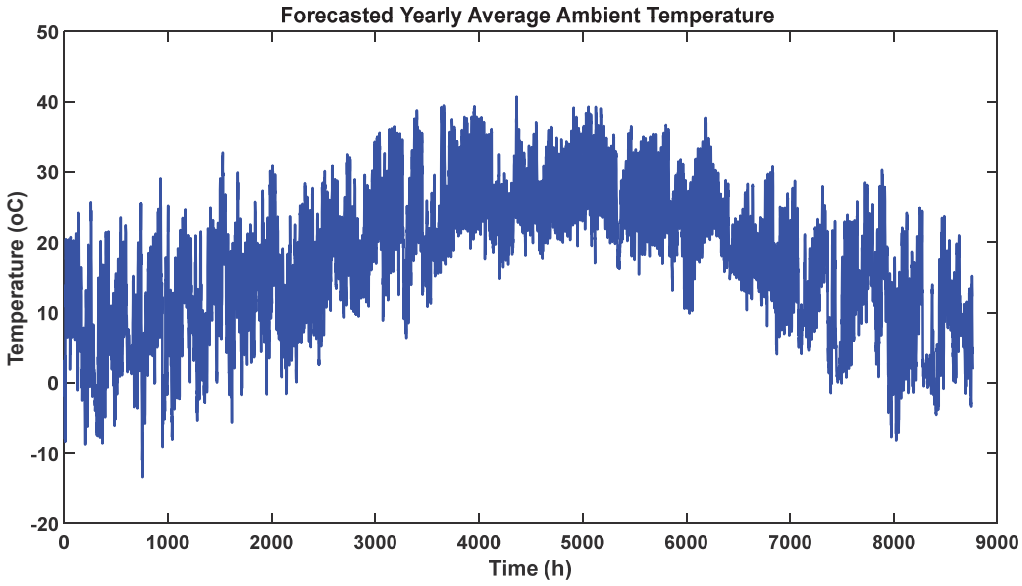

Figure 4-5 Forecasted Yearly Average Ambient Temperature

The forecasted ambient temperature after correction is given in Figure 4-6. The ambient temperature can be less than zero, hence the correction that was applied to the ambient temperature was simply to bring any unfitting or abnormal point into an acceptable range. For instance, if the temperature at the jth hour was 10, then in the forecasted data, it is not expected to be 50. Therefore, this point of temperature must be corrected by setting a limit to the maximum and minimum forecasted data points.

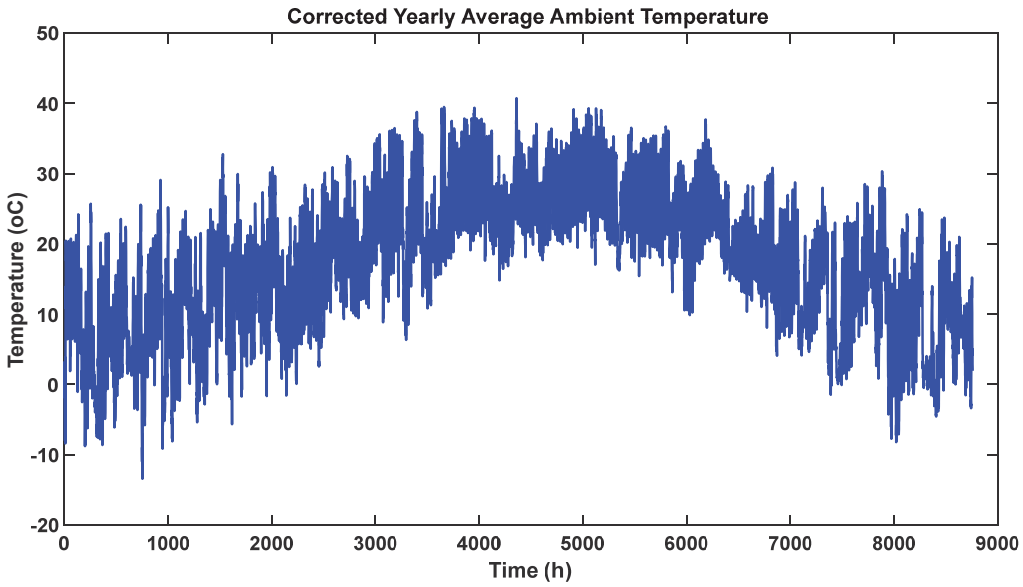

Figure 4-6 Corrected Yearly Average Ambient Temperature

The same scenario that was applied to the solar radiation, and the ambient temperature data is also applied to the wind speed data as shown below.

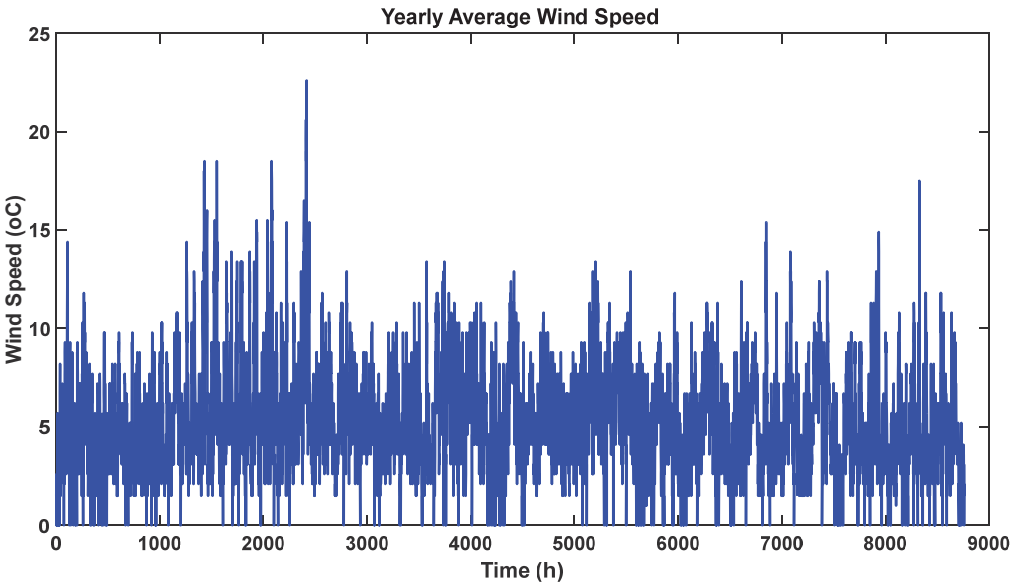

Figure 4-7 Yearly Average Wind Speed

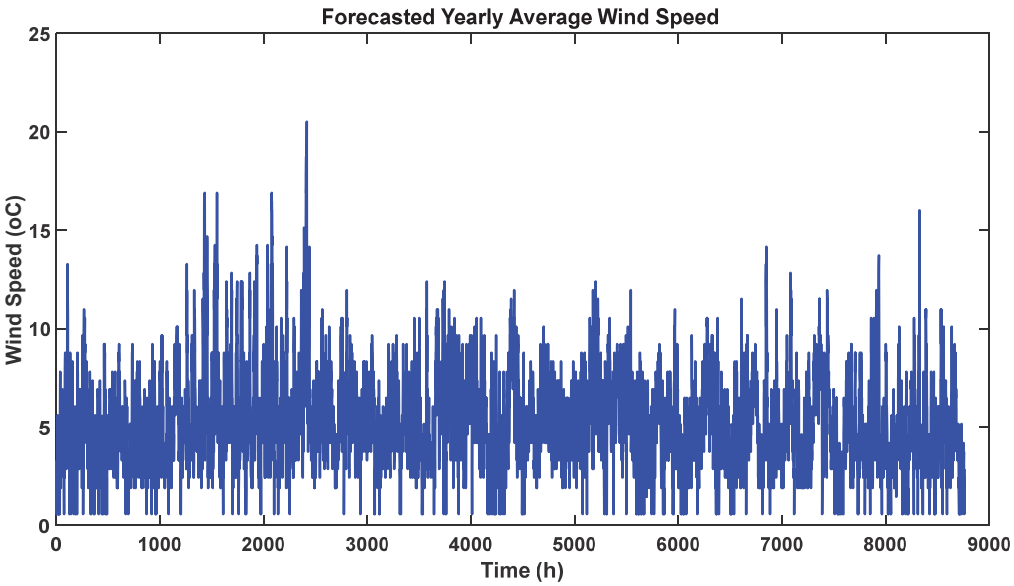

Figure 4-8 Forecasted Yearly Average Wind Speed

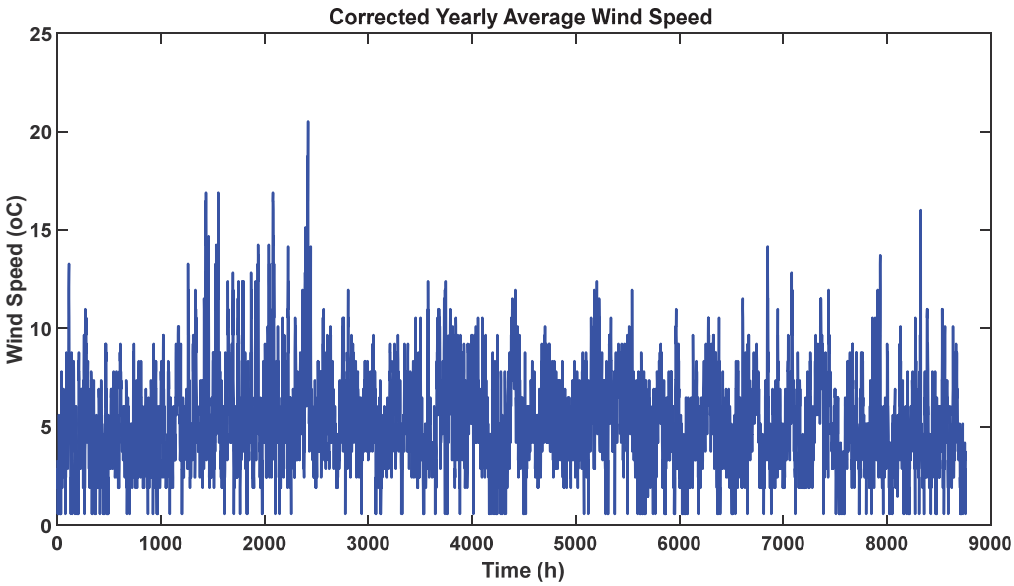

Figure 4-9 Corrected Yearly Average Wind Speed

By using the corrected SR, TEMP and WS, in addition to the data from APPENDIX A INPUT DATA AND PARAMETERS, the solar power (SP) and wind power (WP) can be obtained. The relationship between the wind speed and wind power can also be plotted to assess the quality of the proposed models. The SP, WP, and the wind speed vs. wind power are shown in the following three figures.

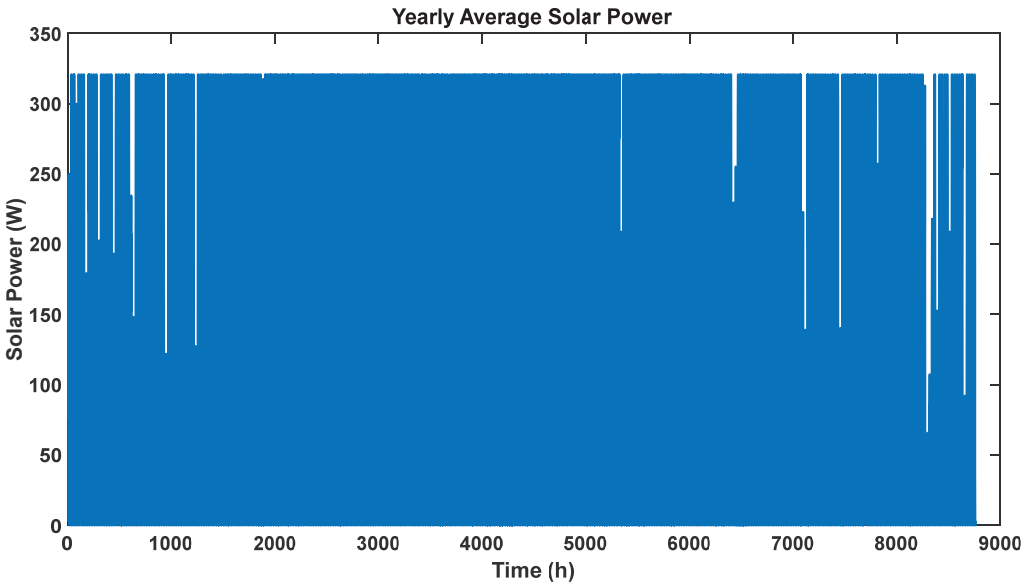

Figure 4-10 Yearly Average Solar Power

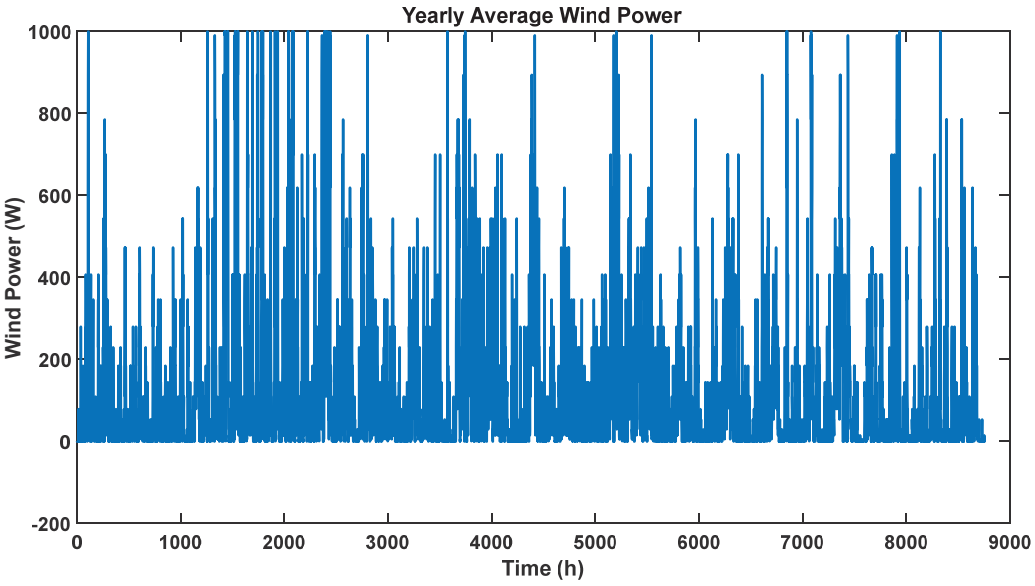

Figure 4-11 Yearly Average Wind Power

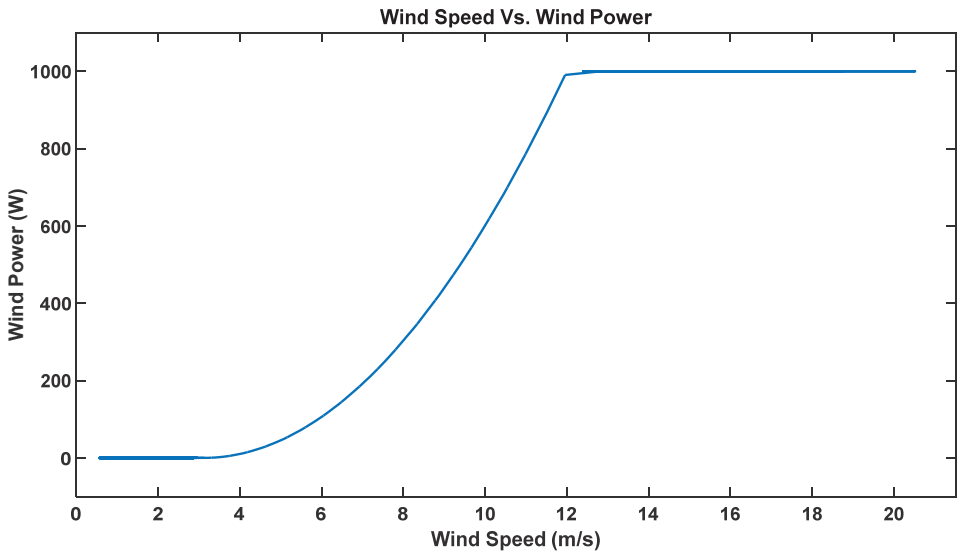

Figure 4-12 Wind Speed Vs. Wind Power

The per-unit residential load data that will be used in this study is provided in Figure 4-13. Nevertheless, the HDGS is applicable to any other load value as desired.

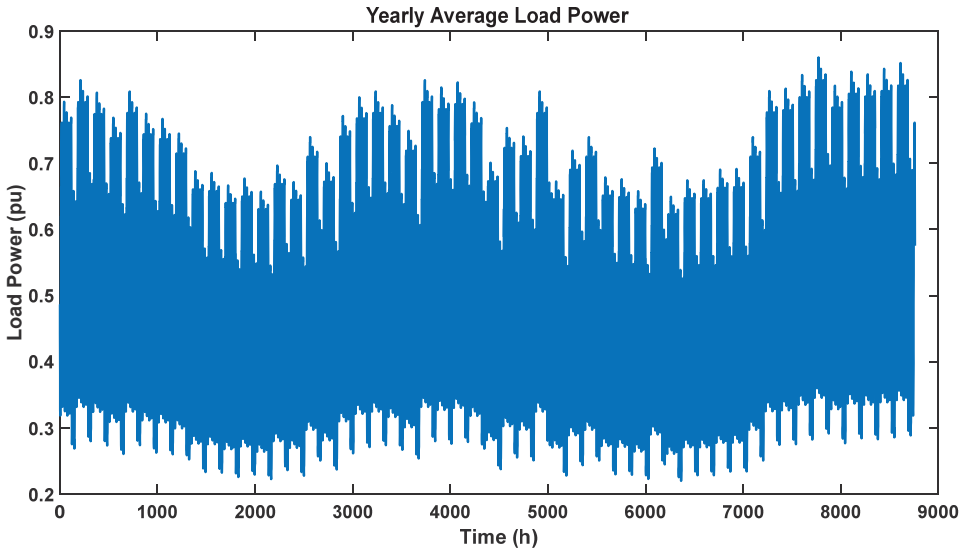

Figure 4-13 Yearly Average Load Power

The load in Figure 4-13 is a per-unit residential load representation. It can be multiplied by any load base value as desired. In this work, the generation and load will be used in their per-unit value based upon one common base value. The main reason for considering all the values per-unit is to generalize the analysis and enable this work to be applied to any case that has different values of demand and/or generation.

4.2 Case Studies

4.2.1 Case 1: Supplying a local load during interruptions

In case 1, the HDGS will supply the local load at the load point where it is installed. When the grid is up, the HDGS will not need to supply the load. If the grid is down, the HDGS will work only for the interruption duration and during all the interruptions that could occur in the study period. When the grid is up, the battery of the HDGS will be allowed to charge from the HDGS. The battery will be assumed to be fully charged at the beginning. The load data as well as the generation data were all presented in the previous set of figures. The representation of case 1 is shown in Figure 4-14. For cases 2 and 3, their representation is provided in Figure 4-15 and Figure 4-16, respectively. The failure rate and repair time at the circuit breaker are 3 failures/year and 9.0287 hours, respectively. The flowcharts shown in Figure 3-5 and Figure 3-6 use the sources in an order that respects the operational cost,

i.e., the renewable sources are used first, then the battery, and lastly the conventional generator if needed.

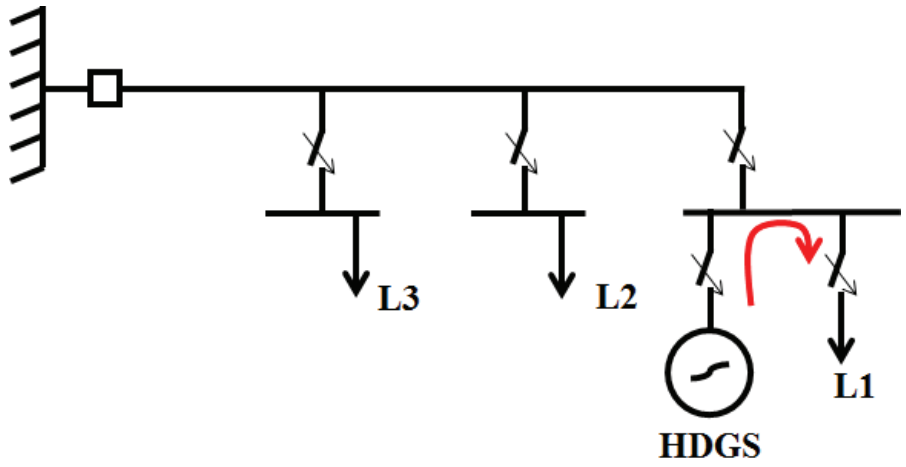

Figure 4-14 Case 1 Representation

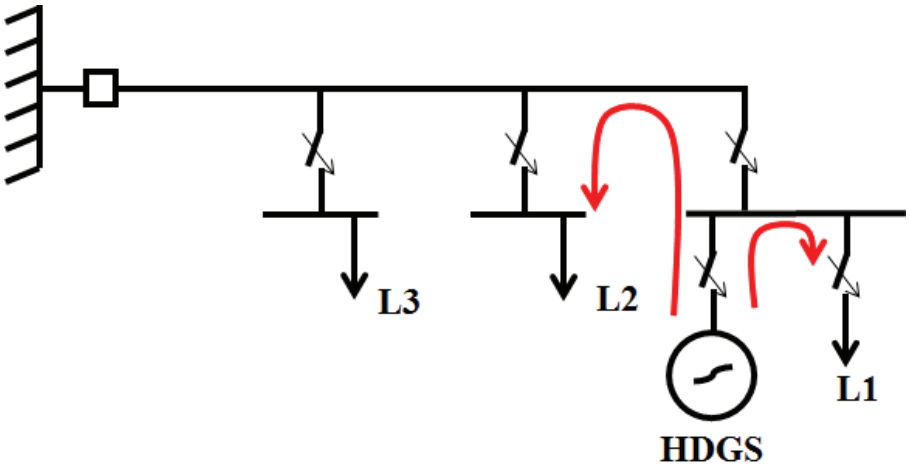

Figure 4-15 Case 2 Representation

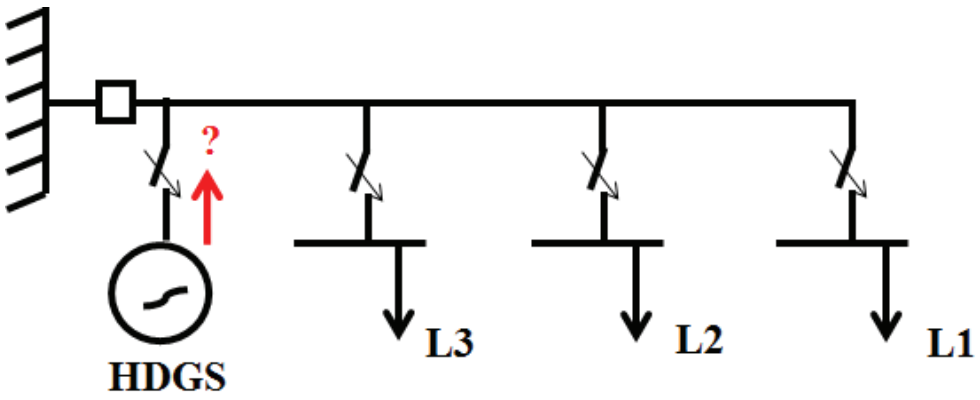

Figure 4-16 Case 3 Representation

The power flow of the different components of the system for case 1 is given in Figure 4-17. The statistical and reliability data during failures are summarized in Table 4-2.

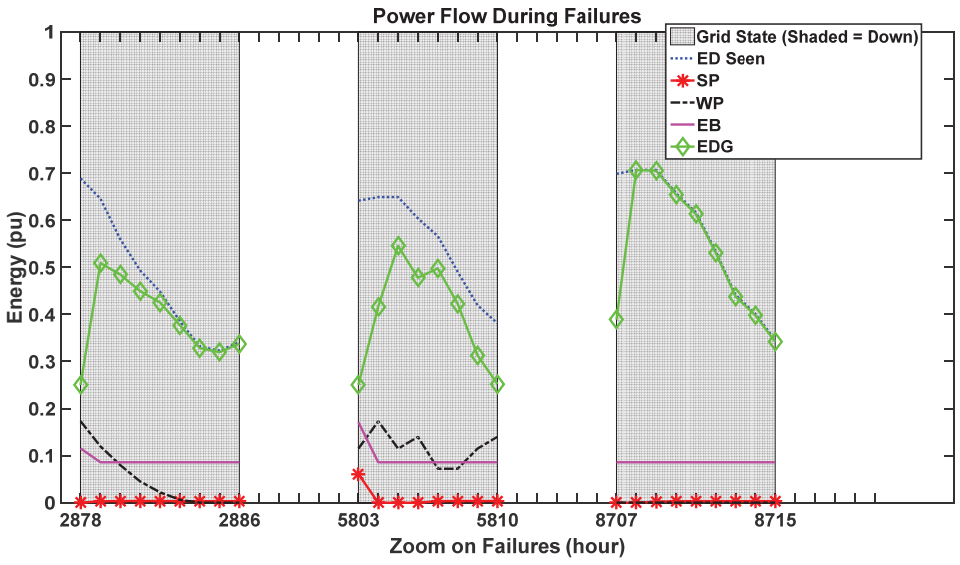

Figure 4-17 Case 1: Power Flow During Failures

In the figure above, the term “ED Seen” stands for the load demanded as seen by the HDGS, and it is shown as a blue dotted line. This denotes that “ED Seen” is not the entire the load of all of the load points. It is simply whatever the HDGS is required to supply at the jth hour. The terms “SP” and “WP” are the PV and wind power, and they are denoted by the red and black lines, respectively. The energy in the battery is denoted by “EB,” which is shown in the figure with a magenta colour. “EDG” is the energy from the diesel generator and is shown in green.

The battery is assumed to start from a fully charged state. However, by looking at the first hour of failure, the 2878th hour in the figure above, it can be noted that the battery is not fully charged. The reason behind this is that the effect of discharge at any hour j is applied at that hour. In other words, at the 2878th hour, the battery was discharged by an amount of energy equal to the difference between the maximum battery charge and the value shown in the figure at the 2878th hour. To explain it in terms of numbers, consider that the battery had an amount of energy of 1 pu at the jth hour and that it was required to discharge an amount of 0.6 pu. As a result, at the jth hour, the battery will be shown in the figure to have 0.4 pu instead of 1 pu.

4.2.2 Case 2: Supplying a local load and a nearby load during interruptions

This is precisely the same situation as case 1 except that, at each hour, if there is some energy left in any of the sources or the storage system, the energy will be supplied to the load at the next load point. However, the battery will not be allowed to discharge for load 2. This is to make certain that the priority of supply will always be given to load 1. Load 2 is taken to be 0.8 of load 1, while load 3, the load next to load 1, is taken to be 0.9 of load 1. The load 1 data were previously provided, and thus, loads two and three can be obtained.

The power flow from/to the different components of the system for case 2 with respect to load 1 are given in Figure 4-18, while the power flow from/to those components with respect to load 2 is shown in Figure 4-19.

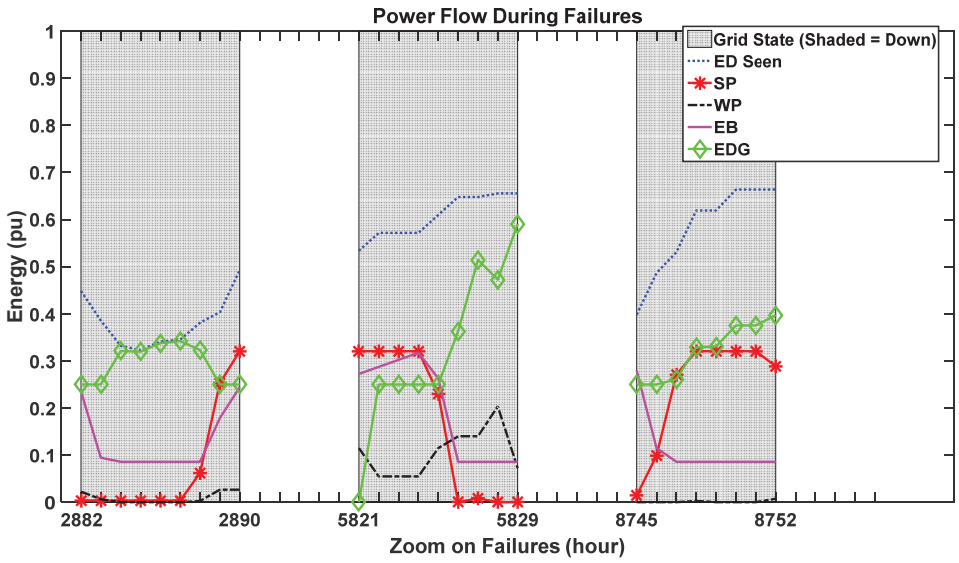

Figure 4-18 Case 2: Power Flow During Failures (Load 1)

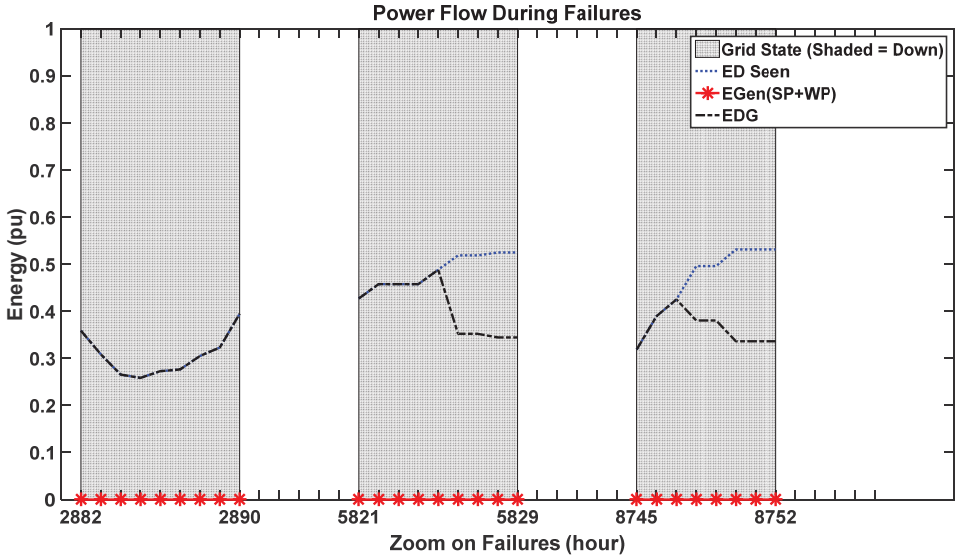

Figure 4-19 Case 2: Power Flow During Failures (Load 2)

In the previous figure, “EGen (SP+WP)” is whatever unused power is left from the renewable resources after feeding load 1. This power will be delivered to the second load, which is called “EGen,” or the generated energy from the renewable resources.

4.2.3 Case 3: Supplying two loads during interruptions based upon a priority list

This is a very similar case to case 2 except that the two loads that will be supplied will not be the local load, load 1, and the load next to it, load 2. The system will be given a priority list specifying which load is more important, which comes second, and which comes third. Then, the HDGS will supply the most important load and provide the remaining energy to the second most important load.

The power flow of the different components of the HDGS in case 3 with respect to the most important load is given in Figure 4-20, while the power flows from/to those components with respect to the second most important load are shown in Figure 4-21. It is worth noting that, in some cases, if the generated power is observed to be more than the demand, this phenomenon is due to the efficiency of the inverter and the battery charging, which scale down the energy generated before it is transferred to the load.

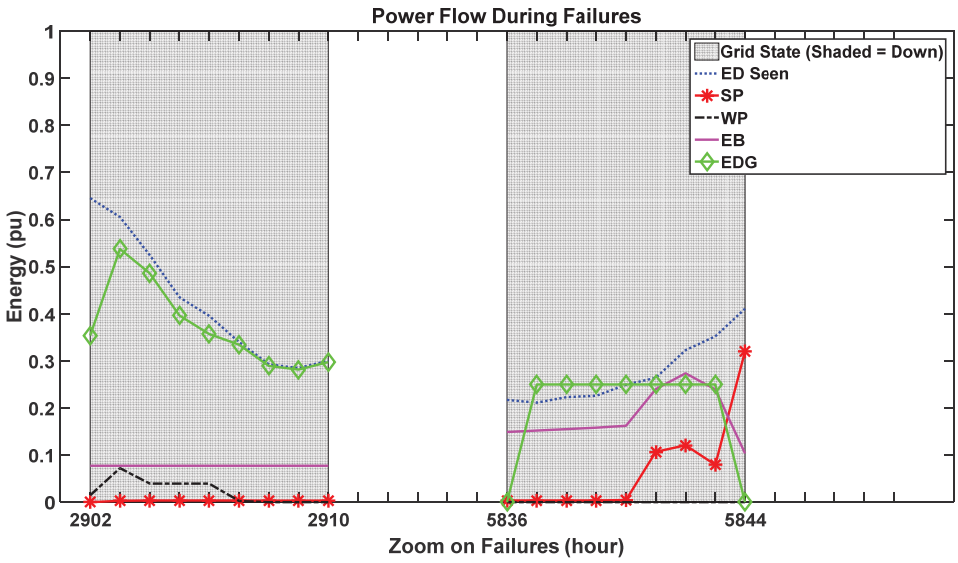

Figure 4-20 Case 3: Power Flow During Failures (Load 1)

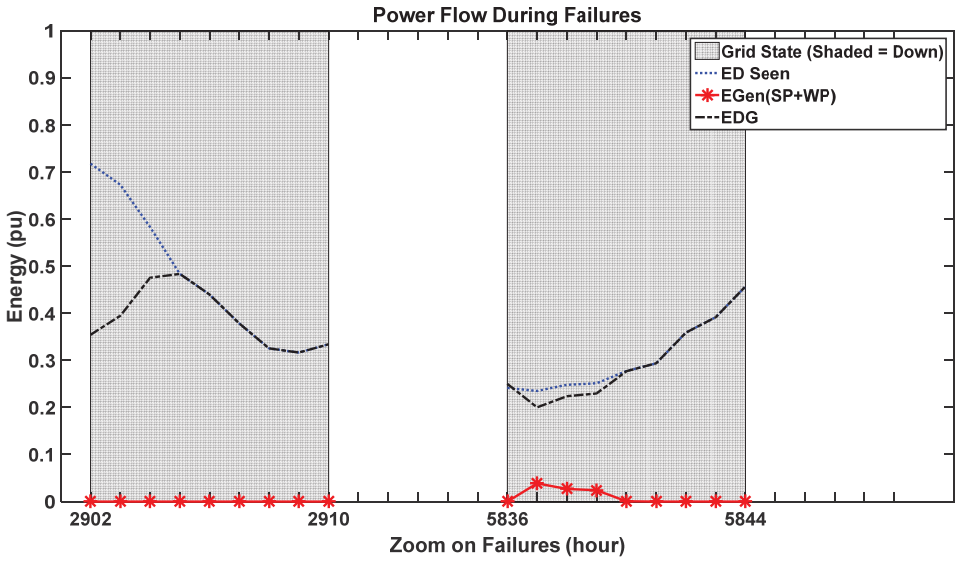

Figure 4-21 Case 3: Power Flow During Failures (Load 2)

Table 4-2 STATISTICAL AND RELIABILITY DATA SUMMARY (DURING FAILURES)

	Case 1	Case 2 (Load 1)	Case 2 (Load 2)	Case 3 (Load 1)	Case 3 (Load 2)
Energy Unused	0	0	0	0.0899	0.0086
Energy Unsatisfied	0	0	1.5087	0	0.7495
Energy Demand	13.7238	13.5669	10.8535	6.3029	7.0032
Energy Supplied	13.7238	13.5669	9.3448	6.3029	6.2537
Energy (PV)	0.1253	4.1327	---	0.674	---
Energy (Wind)	1.3895	1.0451	---	0.2087	---
Energy (CG)	11.4317	8.1526	9.3448	5.0843	6.1814
Energy (Battery)	2.3506	3.8799	---	2.3307	---
Energy (Battery_Min)	2.236	2.236	---	1.3932	---
Energy Generated (PV + Wind)	---	---	0	---	0.0899
LOLP 1	0	0	0.139	0	0.107
LOLP 2	0	0	0.3462	0	0.1667

In Table 4-2, “Energy Unused” is the excess energy that is not used at all for any purpose, and “Energy Unsatisfied” is the part of the demand that could not be met by the HDGS. The numbers in the table represent the summation of the points during all of the study’s interruptions. Therefore, “Energy Unused” represents the summation of the energy unused at every hour of interruption when the HDGS was operated. “Energy Demand” is the total load demand that was required from the HDGS, and “Energy Supplied” is the energy that the HDGS was successfully able to deliver to the load. “Energy (PV),” “Energy (Wind),” and “Energy (CG)” represent the energy produced by the PV, wind, and conventional systems, respectively. “Energy (Battery)” is the total energy left in the battery after

considering all the charging and discharging at every hour of interruption. “Energy Battery_Min” is the total amount of energy that cannot be taken out of the battery during failures, i.e., the number of hours of failure multiplied by the minimum energy of the battery. The “Energy Generated” is simply whatever is left from the PV and wind power from the first load in addition to any power excess that was left. That energy will be available to supply the second load. Thus, the energy generated is not applicable in the case of the first load. In addition, the wind and PV energies are not applicable to the case of the second load as they are lumped into one term, “Energy Generated.” It is worth mentioning that the battery is not allowed to discharge to feed the second load. It serves only the first load. The loss of load probability indices (LOLP 1 and LOLP 2) are provided in the following equations [67]:

$$LOLP\ 1 = \frac{\sum_{i=1}^{n} Energy\ Unsatisfied}{\sum_{i=1}^{n} Energy\ Demand} \tag{4-1}$$

$$LOLP\ 2 = \frac{\sum_{i=1}^{n} u(Energy\ Unsatisfied)}{N} \tag{4-2}$$

where ‘i’ is the hour number and ‘n’ is the last hour of failure. $u(Energy\ Unsatisfied)$ is a step function that is equal to 1 when the unsatisfied energy is positive, and it is otherwise equal to zero. N here represents the total number of hours considered in the study.

In the next case studies, some parameters of the components of the system will be changed, and their effect on the results will be studied. There are numerous parameters that could be changed; however, the focus here will be on two important parameters, namely, the conventional generator's maximum power rating and the battery's size. Those two chosen parameters are selected due to their impact on the behaviour of the system. The renewable resources are intermittent, and therefore, their effect on the overall behaviour is not as critical as the effect of the diesel generator and the battery.

4.2.4 Case 4: The Diesel Generator's Parameter

In this case, the diesel generator's maximum power output will be set to 0.65 pu instead of 1 pu, and none of the other parameters will change in the complete system. The result of this parameter change is provided in Table 4-3. It is important to note that there is no limit set for the LOLP indices. This is because this work studies the effect of sizing the system and does not focus on optimizing or setting a specific size of the HDGS.

Table 4-3 CASE STUDY ANALYSIS (CASE 4)

	Case 1	Case 2 (Load 1)	Case 2 (Load 2)	Case 3 (Load 1)	Case 3 (Load 2)
Energy Unused	0	0	0	0.0055	0
Energy Unsatisfied	0.5359	0.1802	4.4799	0	2.3214
Energy Demand	14.9856	8.9851	7.1881	5.7995	6.4439
Energy Supplied	14.4497	8.8049	2.7083	5.7995	4.1225
Energy (PV)	5.6172	0.4147	---	0.5766	---
Energy (Wind)	0.4572	0.4905	---	0.5457	---
Energy (CG)	8.1249	7.3719	2.7083	4.2868	4.1176
Energy (Battery)	3.1049	1.6527	---	2.1576	---
Energy (Battery_Min)	2.2360	1.462	---	1.2384	---
Energy Generated (PV + Wind)	---	---	0	---	0.0055
LOLP 1	0.0358	0.0201	0.6232	0	0.3602
LOLP 2	0.1538	0.1765	0.8235	0	0.375

4.2.5 Case 5: The Battery's Parameter

In this case, the battery's size will be set to 25% of the maximum demand instead of 50%, and none of the other parameters will change in the complete system. The result of this parameter change is provided in Table 4-4.

Table 4-4 CASE STUDY ANALYSIS (CASE 5)

	Case 1	Case 2 (Load 1)	Case 2 (Load 2)	Case 3 (Load 1)	Case 3 (Load 2)
Energy Unused	0.0964	0	0	0.056	0
Energy Unsatisfied	0	0	1.3509	0	0.4632
Energy Demand	7.14	11.8348	9.4679	8.9378	9.9309
Energy Supplied	7.14	11.8348	8.1169	8.9378	9.4676
Energy (PV)	0.2623	1.1964	---	1.9894	---
Energy (Wind)	0.2386	0.6918	---	0.3619	---
Energy (CG)	6.6513	9.703	8.1169	6.6075	9.4172
Energy (Battery)	1.4891	1.5024	---	1.7837	---
Energy (Battery_Min)	0.731	1.118	---	0.774	---
Energy Generated (PV + Wind)	---	---	0	---	0.056
LOLP 1	0	0	0.1427	0	0.0466
LOLP 2	0	0	0.2308	0	0.25

It can be concluded from Table 4-2, Table 4-3, and Table 4-4 that reducing the battery size to half of the original does not greatly affect the LOLP indices. This is because there exists a large conventional generator in the system that can cover for the lost part of the storage. However, this implies that losing some part of this conventional/diesel generator will significantly disturb the system compared to the case of losing part of the storage. Indeed, the results confirm what the analysis implied. Table 4-3 shows that, in one case, LOLP 2 became 0.8235. Therefore, from a planning point of view, which is beyond the scope of this work, this diesel generator is better optimized in terms of its size.

4.3 Discussion and Analysis

In this section, the case studies and their results will be concisely summarized. Three case studies have been undertaken, and two more cases regarding the effects of changing various parameters were evaluated. For all of the case studies, there were three load points connected radially with one main breaker for the bus that protects all the load points. Resultantly, any fault at any point along any of the three load points will open the circuit breaker at the bus and disconnect the three load points. It makes sense to study a radial system in this case, as distribution systems tend to be general radial systems. When the breaker opens, the three loads will experience a failure.

In case 1, the HDGS will be allowed to supply only the local load at the load point at which it is installed. Of course, this could be any of the three load points, but the HDGS will supply this and only this load point where it is installed. After that, the hourly analysis will be performed to test the reliability of the system at the load point. The reliability is tested through the loss of load probability indices.

In case 2, the HDGS will first have to respond to the demand from the load point at which it is installed. Thereafter, if there is any energy left in any of the energy-generating sources, it will be allowed to feed the load that is at the next load point directly after the load point at which the HDGS is installed. Case 3 will feed two loads, as mentioned in case 2, but this

time, the two loads do not have to be local and neighbouring loads. In fact, the HDGS will be installed right after the bus and circuit breaker and not at any specific load point. Consequently, the HDGS can supply any chosen loads in any order, and this is why a priority list is needed. The system will be given a priority list stating the importance of each load. Based upon that list, the HDGS will feed the most important load first and it will then subsequently feed the second most important load, if possible.

CHAPTER 5

CONCLUSION AND FUTURE WORK

5.1 Conclusion

In conclusion, the wind, PV, conventional, and storage systems have been represented by accurate models. Reliability block diagrams were used to represent the physical components of each of those subsystems. The wind speed, solar radiation and ambient temperature were collected and used to perform sequential hourly forecasting of the future data. The power output of each subsystem was obtained using the input-output mathematical relations of each subsystem. The failure and repair rates of all the components, subsystems, and loads were simulated using the Monte Carlo technique. An effective technique of energy management, locally and on the feeder, was proposed to minimize the operational cost by keeping the conventional generator as the last one to run. A complete HDGS design has been proposed and introduced in this work. Three case studies were presented, and they proved the validity of the proposed HDGS. More case studies were conducted with the system and demonstrated that the conventional generator's size can greatly affect the reliability of the system. This thesis draws on simulation and representation techniques, which distinguishes it from the literature, where mostly only one technique or one subsystem is studied.

5.2 Future Work

It can be observed that the proposed system involves the use of various simulation and analysis techniques. However, the overall scheme was a simulation operational scheme. Thus, even though the failure and repair rates of the components were included and reliability block diagrams were used, the process has been converted to simulation rather than states. The aspects and concerns of possible future work are listed below:

1- This system can be designed using Markov modelling. All of the components can be made into states with transition rates, and these states can be combined to form the complete HDGS.

2- Representing the system by Markov states may increase the complexity and the calculation time.

3- It can be very useful as it becomes handy for reliability studies, depending on the purpose of the study, and it can be compared to the results obtained from this thesis.

APPENDIX A

INPUT DATA AND PARAMETERS

Table A-1 Efficiency and Other Parameters

Component	Efficiency
EBmin	20 %
EBmax	100 %
ηbat	85 %
ηinv	90 %
DOD	80 %

Table A-2 WTG FAILURE RATES AND REPAIR TIMES [19], [39]-[40]

Component	Avg. # Failures /yr.	Avg. Down Time per year (h)	Avg. Down Time per Failure (h)
Entire Unit	0.011	0.8	79.7
Structure	0.006	0.6	104.1
Yaw System	0.026	6.6	259.4
Hydraulics	0.061	2.6	43.2
Mechanical Brakes	0.005	0.6	125.4
Gears	0.045	11.6	256.7
Sensors	0.054	2.7	49.4
Drive Train	0.004	1.2	291.4
Control System	0.05	9.2	184.6
Electric System	0.067	7.2	106.6
Generator	0.021	4.5	210.7
Blades/ Pitch	0.052	4.7	91.6
Hub	0.001	0.000000001 (0)	12.5

Table A-3 PV SYSTEM COMPONENTS' FAILURE AND REPAIR RATES [19],[67]

Component	Failure Rate (Occ./Yr.)	Repair Rate (Occ./Yr.)
Panels	0.004	219
Inverter	0.5	50
Charge Controller	0.125	50
Control Unit	0.1	50
WTG Rectifier	0.5	50

Table A-4 UNITS' COSTS [23]

	Component	Rating/ Performance/ Cost ($)
Wind	Wind Turbine (BWCXL1) Capital Cost/ Salvage Value, pu Annual O&M Cost, pu Life Time	1 KW 3200 $/ 320 $ 100 $ 20 Years
PV	PV Module (SX-120S) Capital Cost/ Salvage Value, pu Annual O&M Cost, pu Life Time	120 W 650 $/ 65 $ 5 $ 20 Years
Diesel Generator	Diesel Generator Capital Cost/ Salvage Value Annual O&M Cost Fuel Cost Life Time	3 KW 550 $/ (55 $ per KW) 0.025 $ per KWh 0.2 $ per KWh 5 Years
Battery	Battery (Deep Cycle) 12 V Capital Cost Annual O&M Cost Life Time/ Efficiency/ DOD	1.35 KWh 100$ (10 $ per KWh) 5 Years/ 85%/80%
Inverter	Inverter Efficiency/ Life	3 KW 95%/ 20 Years
HDGS Project	Project Life Interest Rate Inflation Rate	20 Years 15% 9%

Table A-5 PV SYSTEM'S PARAMETERS [41]

PV Parameters	Unit	Value
Pmpp	W	320
Vmpp	V	54.7
Impp	A	5.86
Voc	V	64.8
Isc	A	6.24
Kv	mV/K	-176.6
Ki	mA/K	3.5
Not	^{o}C	45

Table A-6 WTG SYSTEM'S PARAMETERS [41]

WTG Parameters	Unit	Value
Rated Power	W	500
Rated Speed	m/s	12
Cut-in Speed	m/s	3
Cut-out Speed	m/s	24

Table A-7 CONVENTIONAL DG SYSTEM'S PARAMETERS [41], [68]

Conventional DG Parameters	Unit	Value
Rated Power	W	750
Minimum Power	W	250
MTTF	hours	7500
MTTR	hours	150
Failures per start attempt	(f/start)	0.0135

References

[1] Kroposki, Benjamin, Christopher Pink, Thomas Basso, and Richard DeBlasio. "Microgrid standards and technology development." IEEE in Power Engineering Society General Meeting, 2007, pp. 1-4.

[2] ISC Committee. "IEEE standard for interconnecting distributed resources with electric power systems." IEEE Std. 1547–2003: 1-28.

[3] Andrade, Waltencir S., Carmen LT Borges, and Djalma M. Falcão. "Modeling reliability aspects of distributed generation connected to distribution systems." In Power Engineering Society General Meeting, 2006. IEEE, pp. 6-pp.

[4] Lingfeng, Kou, Sheng Wanxing, Wang Jinyu, Liang Ying, and Song Qipeng. "Evaluation on the application mode of distributed generation." In Electricity Distribution (CICED), 2012 China International Conference on, pp. 1-5.

[5] Abdellatif, Hussein, and Ibrahim El-Amin. "Markov modeling of solar radiation and storage sizing." In GCC Conference and Exhibition (GCCCE), 2015 IEEE 8th, pp. 1-6.

[6] Mohamed, Shaza, and Yasser G. Hegazy. "Wind turbine generator modeling for power production estimation & reliability analysis." In Innovative Smart Grid Technologies (ISGT Europe), 2012 3rd IEEE PES International Conference and Exhibition on, pp. 1-7.

[7] Kakimoto, Naoto, Syo Matsumura, Kaoru Kobayashi, and Mamoru Shoji. "Two-state markov model of solar radiation and consideration on storage size." IEEE Transactions on Sustainable Energy, no. 1 (2014): 171-181.

[8] Giraud, Francois, and Zyiad M. Salameh. "Steady-state performance of a grid-connected rooftop hybrid wind-photovoltaic power system with battery storage." IEEE Transactions on Energy Conversion, no. 1 (2001): 1-7.

[9] Navarro, Antonio, Luis F. Ochoa, and Dan Randles. "Monte Carlo-based assessment of PV impacts on real UK low voltage networks." In Power and Energy Society General Meeting (PES), 2013 IEEE, pp. 1-5.

[10] Maghraby, H. A. M., M. H. Shwehdi, and Ghassan K. Al-Bassam. "Probabilistic assessment of photovoltaic (PV) generation systems." IEEE Transactions on Power Systems, no. 1 (2002): 205-208.

[11] Song J., Krishnamurthy V., Kwasinski A., and R. Sharma, “Development of a Markov-chain-based energy storage model for power supply availability assessment of photovoltaic generation plants,” IEEE Transactions on Sustain Energy, Apr. 2013, vol. 4, no. 2, pp. 491–500.

[12] Lidula, N. W. A., and A. D. Rajapakse. "Microgrids research: A review of experimental microgrids and test systems." Renewable and Sustainable Energy Reviews, no. 1 (2011): 186-202.
[13] Tsuda, Izumi, Sanekazu Igari, Kenji Nakahara, Kiyoshi Takahisa, Kengo Morita, and Hiroshi Kato. "Long term reliability evaluation of PV module." In Photovoltaic Energy Conversion, 2003. Proceedings of 3rd World Conference on, vol. 2, pp. 1960-1963.
[14] Koh, L. H., Gao Zhi Yong, Wang Peng, and K. J. Tseng. "Impact of energy storage and variability of PV on power system reliability." Energy Procedia (2013): 302-310.
[15] Gafurov, Tokhir, Milan Prodanovic, and Julio Usaola. "PV system model reduction for reliability assessment studies." In Innovative Smart Grid Technologies Europe (ISGT EUROPE), 2013 4th IEEE/PES, pp. 1-5.
[16] Miller, Steven P., Jennifer E. Granata, and Joshua S. Stein. The Comparison of Three Photovoltaic System Designs Using the Photovoltaic Reliability and Performance Model (PV-RPM), 2012, No. SAND2012-10342. Sandia National Laboratories (SNL-NM), Albuquerque, NM (United States).
[17] Cha, Seung-Tea, Dong-Hoon Jeon, In-Su Bae, Il-Ryong Lee, and Jin-O. Kim. "Reliability evaluation of distribution system connected photovoltaic generation considering weather effects." In Probabilistic Methods Applied to Power Systems, 2004 International Conference on, pp. 451-456.
[18] Dhople, Sairaj V., Ali Davoudi, Patrick L. Chapman, and Alejandro D. Domínguez-García. "Integrating photovoltaic inverter reliability into energy yield estimation with Markov models." In Control and Modeling for Power Electronics (COMPEL), 2010 IEEE 12th Workshop on, pp. 1-5.
[19] Lalitha, M. Padma, P. Harshavardhan Reddy, and P. Janardhana Naidu. "Reliability evaluation of wind and PV energy penetrated power system." In Reliability, Infocom Technologies and Optimization (ICRITO) (Trends and Future Directions), 2014 3rd International Conference on, pp. 1-5.
[20] Mohamed, Shaza, and Yasser G. Hegazy. "Wind turbine generator modeling for power production estimation & reliability analysis." In Innovative Smart Grid Technologies (ISGT Europe), 2012 3rd IEEE PES International Conference and Exhibition on, pp. 1-7.
[21] Wu, Liang, Jeongje Park, Jaeseok Choi, A. A. El-Keib, Mohammad Shahidehpour, and Roy Billinton. "Probabilistic reliability evaluation of power systems including wind turbine generators using a simplified multi-state model: A case study." In Power & Energy Society General Meeting, 2009. PES'09. IEEE, pp. 1-6.
[22] Dobakhshari, Ahmad Salehi, and Mahmud Fotuhi-Firuzabad. "A reliability model of large wind farms for power system adequacy studies." IEEE Transactions on Energy Conversion, , no. 3 (2009): 792-801.

[23] Gupta, S. C., Y. Kumar, and Gayatri Agnihotri. "Optimal sizing of solar-wind hybrid system." (2007): 282-287.
[24] Karki, Rajesh, Po Hu, and Roy Billinton. "A simplified wind power generation model for reliability evaluation." IEEE Transactions on Energy conversion, no. 2 (2006): 533-540.
[25] Allan, R. N. "Reliability evaluation of power systems. "Springer Science & Business Media, 2013.
[26] Allan, Ronald N., Roy Billinton, I. Sjarief, L. Goel, and K. S. So. "A reliability test system for educational purposes-basic distribution system data and results." IEEE Transactions on Power Systems, no. 2 (1991): 813-820.
[27] Billinton, Roy. "A sequential simulation method for the generating capacity adequacy evaluation of small stand-alone wind energy conversion systems." Canadian Conference on Electrical and Computer Engineering, 2002. IEEE CCECE 2002, vol. 1, pp. 72-77.
[28] Billinton, Roy, Hua Chen, and R. Ghajar. "Time-series models for reliability evaluation of power systems including wind energy." Microelectronics Reliability, no. 9 (1996): 1253-1261.
[29] Karki, Rajesh, and Roy Billinton. "Cost-effective wind energy utilization for reliable power supply." IEEE Transactions on Energy Conversion, no. 2 (2004): 435-440.
[30] Koh, L. H., Gao Zhi Yong, Wang Peng, and K. J. Tseng. "Impact of energy storage and variability of PV on power system reliability." Energy Procedia (2013): 302-310.
[31] Gafurov, Tokhir, Milan Prodanovic, and Julio Usaola. "PV system model reduction for reliability assessment studies." In Innovative Smart Grid Technologies Europe (ISGT EUROPE), 2013 4th IEEE/PES, pp. 1-5.
[32] Cha, Seung-Tea, Dong-Hoon Jeon, In-Su Bae, Il-Ryong Lee, and Jin-O. Kim. "Reliability evaluation of distribution system connected photovoltaic generation considering weather effects." International Conference on Probabilistic Methods Applied to Power Systems, 2004, pp. 451-456.
[33] Appendix A's Solar Radiation Data Retrieved from http://www.jsdi.or.jp/~ (2015).
[34] Zahedi, Ahmad. "Performance evaluation of wind turbine using Monte Carlo method and turbine power curve." In IPEC, 2012 Conference on Power & Energy, pp. 161-165.
[35] Kishore, L. Nanda, and E. Fernandez. "Reliability well-being assessment of PV-wind hybrid system using Monte Carlo simulation." International Conference on Emerging Trends in Electrical and Computer Technology (ICETECT), 2011, pp. 63-68.
[36] Ghahderijani, Mohammad Moradi, S. Masoud Barakati, and Saeed Tavakoli. "Reliability evaluation of stand-alone hybrid microgrid using Sequential Monte Carlo

Simulation." Iranian Conference on Renewable Energy and Distributed Generation (ICREDG), 2012 Second, pp. 33-38.
[37] Askari, M. T., M. Z. A. Ab Kadir, H. Hizam, and J. Jasni. "On the selection of wind turbine generator based on ARMA time series." IEEE Conference on Sustainable Utilization and Development in Engineering and Technology (CSUDET), 2013, pp. 42-45.
[38] Billinton, Roy, Hua Chen, and R. Ghajar. "Time-series models for reliability evaluation of power systems including wind energy." Microelectronics Reliability, no. 9 (1996): 1253-1261.
[39] Ribrant, Johan, and Lina Bertling. "Survey of failures in wind power systems with focus on Swedish wind power plants during 1997-2005." In Power Engineering Society General Meeting, 2007. IEEE, pp. 1-8.
[40] Maaref, Mahdi, Hasan Monsef, and Maziar Karimi. "A Reliability Model for a Doubly Fed Induction Generator Based Wind Turbine Unit Considering Auxiliary Components." Indian Journal of Science and Technology, no. 9 (2013): 5281-5288.
[41] Bernardo, Félix Manuel Lorenzo. "Computer Tool for Power Generation Modeling and Economic Analysis for Nearly-Zero Energy Buildings." PhD diss., Universidad de Oviedo, 2014.
[42] Jonnavithula, Annapoorani. Composite system reliability evaluation using sequential Monte Carlo simulation. 1997.
[43] Sankarakrishnan, A., and Roy Billinton. "Sequential Monte Carlo simulation for composite power system reliability analysis with time varying loads." IEEE Transactions on Power Systems, no. 3 (1995): 1540-1545.
[44] Wang, Peng, and Roy Billinton. "Time sequential distribution system reliability worth analysis considering time varying load and cost models." IEEE Transactions on Power Delivery, no. 3 (1999): 1046-1051.
[45] "1991- 2005 Update: Typical Meteorological Year 3." National Solar Radiation Data Base. 2015. Web. 21 Oct. 2015.
http://rredc.nrel.gov/solar/old_data/nsrdb/1991-2005/tmy3/
[46] Wang, Zhu, Rui Yang, Lingfeng Wang, and Jun Tan. "Reliability assessment of integrated residential distribution and PHEV systems using Monte Carlo simulation." In Power and Energy Society General Meeting (PES), 2013 IEEE, pp. 1-5.
[47] Alexander, Dennis. "Application of Monte Carlo simulations to system reliability analysis." In Proceedings of the Twentieth International Pump Users Symposium, pp. 91-94. 2003.
[48] Heydt, Gerald Thomas. "The next generation of power distribution systems." IEEE Transactions on Smart Grid, no. 3 (2010): 225-235.

[49] Yu, Xinghuo. "Interplay of smart grids and intelligent systems and control." In Power Engineering, International Conference on Energy and Electrical Drives (POWERENG), 2011 pp. 1-1.
[50] Xu, Yuzhe, and Carlo Fischione. "Real-time scheduling in LTE for smart grids." International Symposium on Communications Control and Signal Processing (ISCCSP), 2012 5th, pp. 1-6. IEEE, 2012.
[51] Rietveld, Gert, P. John Clarkson, Paul S. Wright, Umberto Pogliano, Johannes Braun, Miha Kokalj, Rado Lapuh, and Norbert Zisky. "Measurement infrastructure for observing and controlling smart electrical grids." In Innovative Smart Grid Technologies (ISGT Europe), 2012 3rd IEEE PES International Conference and Exhibition on, pp. 1-8.
[52] Hashmi, M., S. Hänninen, and K. Mäki. "Survey of smart grid concepts, architectures, and technological demonstrations worldwide." In Innovative Smart Grid Technologies (ISGT Latin America), 2011 IEEE PES Conference on, pp. 1-7.
[53] Al-Muhaini, Mohammad, Gerald T. Heydt, and Anthony Huynh. "The reliability of power distribution systems as calculated using system theoretic concepts." In Power and Energy Society General Meeting, 2010 IEEE, pp. 1-8.
[54] Al-Muhaini, Mohammad, and Gerald T. Heydt. "Evaluating future power distribution system reliability including distributed generation." IEEE Transactions on Power Delivery, no. 4 (2013): 2264-2272.
[55] Al-Muhaini, Mohammad, and Gerald T. Heydt. "A novel method for evaluating future power distribution system reliability." IEEE Transactions on Power Systems, no. 3 (2013): 3018-3027.
[56] Al-Muhaini, Mohammad, and Gerald T. Heydt. "Customized reduction techniques for power distribution system reliability analysis." In Power and Energy Society General Meeting (PES), 2013 IEEE, pp. 1-5.
[57] Nasrolahpour, Ehsan, Meysam Doostizadeh, and Hassan Ghasemi. "Optimal management of micro grid in restructured environment." In Renewable Energy and Distributed Generation (ICREDG), 2012 Second Iranian Conference on, pp. 116-120.
[58] Koutsoumpas, Vasileios, and Pragya Kirti Gupta. "Towards a constraint based approach for Self-Healing Smart Grids." International Workshop on Software Engineering Challenges for the Smart Grid (SE4SG), 2013 2nd, pp. 17-24.
[59] Barker, Philip P., and Robert W. De Mello. "Determining the impact of distributed generation on power systems. I. Radial distribution systems." In Power Engineering Society Summer Meeting, 2000. IEEE, vol. 3, pp. 1645-1656.
[60] McDermott, Thomas E., and Roger C. Dugan. "PQ, reliability and DG." Industry Applications Magazine, IEEE, no. 5 (2003): 17-23.

[61] Brown, Richard E., and Lavelle AA Freeman. "Analyzing the reliability impact of distributed generation." In Power Engineering Society Summer Meeting, 2001, vol. 2, pp. 1013-1018.
[62] Sagar, E. Vidya, and P. V. N. Prasad. "Impact of DG on radial distribution system reliability." energy 102 (2008): pp. 5.
[63] Wei, Huang, He Zijun, Feng Li, Tian Hongliang, and Zhang Li. "Reliability evaluation of Microgrid with PV-WG hybrid system." International Conference on Electric Utility Deregulation and Restructuring and Power Technologies (DRPT), 2011 4th, pp. 1629-1632.
[64] Costa, Paulo Moisés, and Manuel Matos. "Reliability of distribution networks with microgrids." In Power Tech, 2005 IEEE Russia, pp. 1-7.
[65] Bae, In-Su, and Jin-O. Kim. "Reliability evaluation of customers in a microgrid." IEEE Transactions on Power Systems, no. 3 (2008): 1416-1422.
[66] Kwasinski, Alexis, Vaidyanathan Krishnamurthy, Junseok Song, and Ratnesh Sharma. "Availability evaluation of micro-grids for resistant power supply during natural disasters." IEEE Transactions on Smart Grid, no. 4 (2012): 2007-2018.
[67] Theristis, Marios, and Ioannis Papazoglou. "Markovian Reliability Analysis of Standalone Photovoltaic Systems Incorporating Repairs." IEEE Journal of Photovoltaics, no. 1 (2014): 414-422.
[68] Heising, C. "IEEE recommended practice for the design of reliable industrial and commercial power systems." IEEE Inc., New York (2007).

Vitae

Name: HUSSEIN ADEL ABDELAZIM ABDELLATIF

Nationality: EGYPTIAN

Date of Birth: 4/17/1991

Email: hosain96@hotmail.com

Address: KFUPM, P. O. Box 277, Dhahran 31261, Saudi Arabia

Academic Background: Electrical Engineering M. Sc. Jan. 2016, KFUPM - GPA (3.900 out of 4.0)

Electrical Engineering B. Sc. May 2013, KFUPM - GPA (3.942 out of 4.0)

- Published a conference paper in IEEExplore under the title “Markov Modeling of Solar Radiation and Storage Sizing” with prof. Ibrahim El-Amin.
- Research Assistant at KFUPM: Jan. 2014 to May 2016
- IEEEXTREME 9.0 Ambassador: 2015
- Educational videos Translator: Dec. 2011 to Dec. 2013
- Educational Game Content Developer: Mar. 2013 to May 2013
- Grader at KFUPM at the Physics Department: 2011 to 2013
- Summer Trainee at Schlumberger: Jun. 2012 to Aug. 2012
- Grader at KFUPM at the Physics Department: 2009 to 2011